Assessing Computational Methods and Science Policy in Systems Biology

by

Andrea R. Castillo

B.S. Electrical Engineering and Computer Engineering,
Minor Computer Science
Carnegie Mellon University 2005

Submitted to the Engineering Systems Division
in partial fulfillment of the requirements for the degree of

Master of Science in Technology and Policy

at the

MASSACHUSETTS INSTITUTE OF TECHNOLOGY

June 2009

Author .....
Engineering Systems Division
May 8, 2009

Certified by .....
Bruce Tidor
Professor of Biological Engineering and Computer Science
Thesis Supervisor

Accepted by .....
Dava Newman
Professor, Aeronautics and Astronautics and Engineering Systems
Director, Technology and Policy Program

Assessing Computational Methods and Science Policy in Systems Biology

by

Andrea R. Castillo

Submitted to the Engineering Systems Division
on May 8, 2009, in partial fulfillment of the
requirements for the degree of
Master of Science in Technology and Policy

Abstract

In this thesis, I discuss the development of systems biology and issues in the progression of this science discipline. Traditional molecular biology has been driven by reductionism with the belief that breaking down a biological system into the fundamental biomolecular components will elucidate such phenomena. We have reached limitations with this approach due to the complex and dynamical nature of life and our inability to intuit biological behavior from a modular perspective [37].

Mathematical modeling has been integral to current system biology endeavors since detailed analysis would be invasive if performed on humans experimentally or in clinical trials [17]. The interspecies commonalities in systemic properties and molecular mechanisms suggests that certain behaviors transcend specie differentiation and therefore easily lend to generalizing from simpler organisms to more complex organisms such as humans [7, 17].

Current methodologies in mathematical modeling and analysis have been diverse and numerous, with no standardization to progress the discipline in a collaborative manner. Without collaboration during this formative period, successful development and application of systems biology for societal welfare may be at risk. Furthermore, such collaboration has to be standardized in a fundamental approach to discover generic principles, in the manner of preceding long-standing science disciplines.

This study effectively implements and analyzes a mathematical model of a three-protein biochemical network, the *Synechococcus elongatus* circadian clock. I use mass action theory expressed in kronecker products to exploit the ability to apply numerical methods—including sensitivity analysis via boundary value formulation (BVP) and trapiezoidal integration rule—and experimental techniques—including partial reaction fitting and enzyme-driven activations—when mathematically modeling large-scale biochemical networks. Amidst other applicable methodologies, my approach is grounded in the law of mass action because it is based in experimental data and

biomolecular mechanistic properties, yet provides predictive power in the complete delineation of the biological system dynamics for all future time points.

The results of my research demonstrate the holistic approach that mass action methodologies have in determining emergent properties of biological systems. I further stress the necessity to enforce collaboration and standardization in future policymaking, with reconsiderations on current stakeholder incentive to redirect academia and industry focus from new molecular entities to interests in holistic understanding of the complexities and dynamics of life entities. Such redirection away from reductionism could further progress basic and applied scientific research to embetter our circumstances through new treatments and preventive measures for health, and development of new strains and disease control in agriculture and ecology [13].

Thesis Supervisor: Bruce Tidor
Title: Professor of Biological Engineering and Computer Science

Acknowledgments

This study was fulfilled due to the collaborations and contributions of A. Katharina Wilkins, Jared E. Toettcher, and Jacob K. White. I am especially grateful to my thesis supervisor, Bruce Tidor, for his invaluable perspective, direction, and support.

Contents

List of Figures

List of Tables

Chapter 1

Introduction

1.1 Systems Biology Overview

Modern biology explains living beings to be highly organized and complex material entities composed fundamentally of molecules due to a long process of evolution and replication [10]. Life is one of the most complex phenomena known in the universe [26]. Systems biology is an integrative study of life by (1) investigating cellular components and molecular interactions, (2) applying experimental and computational techniques, and (3) analyzing complex interactions to discover new emergent properties that may arise from a systematic and holistic paradigm. Systems biology draws upon all areas of biology and natural science [8] to quantitatively assess the dynamic interactions between several entities of a biological system [9]. In traditional molecular biology, there has been a certain tradition in the reductionist method of dissecting biological systems into their constituent entities as an effective way to explain biological processes. Limitations in this approach are that biological systems are extremely complex and dynamical, having emergent behaviors that are nonintuitive and unexplainable by studying their constituent entities alone [37]. Therefore, systems biology aims to understand emergent behaviors of the system holistically as opposed to the constituent entities singularly [9].

Yet expectations of systems biology are still unclear. Experts in the field visualize the

origin and methodological foundations for systems biology (1) in the accumulation of detailed knowledge with the prospect to advance current practices in biotechnology and health care, (2) in the emergence of new experimental techniques and framework design, (3) in mathematical modeling principled in controls theory, systems theory, and current biological understanding, (4) in the development of computational methods to address high-throughput and resource-intensive analysis, and (5) in the internet as the medium for quick and comprehensive exchange of information [26].

Systems biology is driven by curiosity of scientists and engineers, but even more so by the prospect of its applications to predict the outcome of complex processes. Currently the discipline is still in its formative period, lacking a systematic approach to modeling biochemical networks and signaling pathways in such a way that establishes experimentally testable quantitative predictions despite the complex nature of systems biology models, not to mention the complexity of the underlying biology. The synthesizing of experimentation with theory in systems biology models has been a *modus vivendi* to the discipline. A principled and fundamental approach to the experimentation, mathematical modeling, and quantification is crucial for further successful development of biological science [26].

Systems biology, a new mathematical and computational science, has the joint objectives of reducing experimental and clinical treatment costs, and rapidly advancing current knowledge of biological systems [3]. The integrative approach of systems biology provides 'sufficiently accurate and detailed' models which allow biologists to accomplish the following tasks not possible by traditional biology research: prediction of biological system behavior given an perturbation and knock-out or redesign of biochemical networks to create completely new nonintuitive emergent biological system properties [1]. Being that systems biology lacks a foundational and systematic approach across wet- and dry-labs, current collaborative efforts to progress the discipline have been demanding, and thus matching investment into new theoretical methods is required.

1.2 Significance of this Study

Standardization of systems biology principles can lead to practical use in a complementary technology, synthetic biology, which is to design new and improved biological functions [4]. There are significant implications of this synergy for health (through development of new treatments and new preventive measures), and agriculture and ecology (through development of new strains and disease controls) [13].

In order to better understand biological systems, perturbation of these systems enables us to analyze how emergent behaviors occur. Such analysis cannot be easily or ethically performed on humans experimentally; thus, model organisms provide the approach of choice [17]. The Human Genome and prior studies have inspired current efforts in biology by the observation that different species have many systemic properties and molecular mechanisms in common. This might be the result of ancestral relationships and evolutionary dynamics of life in all living organisms due to similarities in genetic code, metabolic and pathways, molecular machinery. Interspecies commonalities suggest that all life arose from a single common ancestor and leads to predictive power in the fundamental understanding of biological systems that transcends specie differentiation [7, 17]. Thus it is a common practice to generalize from the simpler organisms to more complex organisms such as humans [17].

Chapter 2

Background

2.1 Current Methods

The practical application of computational simulation to systems biology has transitioned biology and related applied research away from being purely descriptive science to being a predictive science [18]. Such modeling is most useful when it (1) produces useful predictions, (2) matches experimental results, (3) generates data at a granularity beyond present-day experimental capabilities, (4) yield nonintuitive insights of the system behavior, (5) identify uncertain components, functions or processes in a system, and (5) perform computational experiments to save time, cost, and effort [27].

Besides the enormous challenge for integrating different levels of information pertaining to genes, mRNAs, proteins, and pathways, a more immediate and fundamental barrier to systems biology progress is in defining a principle approach to modeling methodologies, in developing powerful analyses, and in integrating this information into experimental strategies in order to make discoveries [18]. In contrast to long-standing engineering disciplines, there is a relative inadequacy of software and methods currently available and standardized for analyzing biological circuits. The multitude and diversity of approaches to computational simulation is extensive, including ordinary differential equations, stochastic differential equations, partial differential equations, power law equations, petri nets, cellular automata, and agent-based mod-

els [27].

Systems biology is a science; as a science, it should aim to discover generic principles [7]. System-level understanding necessitates a foundation of principles and methodologies that couple molecular mechanism to biological system behavior [25]. Considering an appropriate level of complexity between abstraction and detail, mathematical models should be designed to synthesize and transform information into insight.

Experts in the field have stressed the necessity for widespread standard notation of theoretical frameworks and tools for integrating information, displaying models graphically, and mathematical modeling and simulation of biological system. The integration of technology, biology, and computation is a commanding challenge to basic and applied systems biology research, for both academia and industry. Such an initiative towards standardization would enable studies at different institutions to directly exchange their fully detailed mathematical models [18].

2.2 Contributions

The progress and societal contributions of systems biology depend decisively on the collaborative development of modeling complex systems [9]. A major motivation of current work is the analysis of biochemical networks including gene networks, protein interaction networks, metabolic networks, and signaling networks. The presence of biological uncertainties have driven researchers to study more realistic and detailed models in order to understand these biological phenomenas. Currently there is no standard formulation for these biochemical networks, and therefore an array of mathematical modeling techniques and analytical methods have been implemented in attempt to figure out what works. In this study we propose a formulation of a

three-protein interaction network, the *Synechococcus elongatus* circadian clock, using mass action theory expressed in kronecker products. Such formulation may exploit the simple algebraic manipulation of large-scale biochemical networks and serve as a basis for efficient and general application of methods [5, 12].

The understanding of the structural-functional relationships of molecules have evolved due to the capability of quantifying the law of mass action dynamics in systems biology models [43]. The law of mass action, introduced by Guldberg and Waage in the nineteenth century, is a powerful and well-established concept that descibes the average behavior of a dynamical and complex system. Specifically it states that the rate of a reaction is proportional to the probability of interaction of the reactants. This probability, in turn, is proportional to the concentrations of the reactants to the stochiometry, the power of the molecularity. Implicit in the 'proportionality' aspect of this Law is an assumption that the quantities concerned in inducing interactions and transitions are in a homogeneous solution. The phenomenology of this Law can, in principle, be derived from statistical mechanics and quantum mechanics, although it is regarded as accurate due to the wealth of experimental information on a varity of biological, chemical and physical science based theories that assume it [41].

This approach incorporates structural and biophysical properties of the constituent molecules by modeling the resulting molecular mechanism. Therefore, given knowledge of initial species concentrations, which is an entity of one or more molecules, and parameterization of how these molecules interact, the law of mass action provides a complete delineation of the biological system dynamics at all future time points. We denote the concentration of the reactants by lower case letters

$$s = [S], \quad e = [E], \quad c = [S : E], \quad p = [P]$$

where the concentration is traditionally denoted in the brackets. The biological system dynamics is represented schematically by

$$S + E \underset{k_{-1}}{\overset{k_1}{\rightleftharpoons}} S : E \xrightarrow{k_2} P + E.$$

where the reactions occur at an associate rate parameter constant, in this case k_1, k_{-1} or k_2, and the double-stacked arrows indicate a reversible reaction and the single arrow an irreversible reaction. The example mechanism provided here is the conversion of a substrate S, by catalysis of an enzyme E, into a product P. The stochiometry of this system is one, where one molecule of S combines with one molecule of E to form a two molecule $S : E$ complex, which eventually produces one molecule of P and one molecule of E. The law of mass action, applied to the above set of reactions leads to an equation per each reactant, and hence the system of ordinary differential equation (ODE) system for nonlinear reactions as follows

$$\frac{d[S]}{dt} = -k_1 \cdot [E] \cdot [S] + k_{-1} \cdot [S : E],$$

$$\frac{d[E]}{dt} = -k_1 \cdot [E] \cdot [S] + (k_{-1} + k_2) \cdot [S : E],$$

$$\frac{d[S : E]}{dt} = k_1 \cdot [E] \cdot [S] - (k_{-1} + k_2) \cdot [S : E],$$

$$\text{and} \quad \frac{d[P]}{dt} = k_2 \cdot [S : E].$$

The reaction rate constants, represented as the k's, are the constants of proportionality in the application of the law of mass action [30]. To implement a time series simulation, the initial conditions, which are those at the start of the process which converts S to P, must be set for the concentration of the reactants.

To efficiently simulate an example biochemical network and compute numerical methods on nonlinear ODE models, I have implemented mass action kinetic modeling in Kronecker product formulation [5] to assess principle methods of mass action modeling and analysis in systems biology. Emphasis was placed on assessing the objectivity

of this approach and how this approach affects interpretation and definition of the biochemical network behavior. From a scientific perspective, the goal was to determine emergent properties of the system utilizing the mathematical modeling proposed here. Although the mathematical modeling is part of an iterative model design cycle including feedback from proposed experimental frameworks [9], this study was an effort to determine the advantage of grounding systems biology approaches in the foundational theory of mass action dynamics and computational representation in the Kronecker product.

Chapter 3

Analysis of the Autonomic Protein Oscillation from *Synechococcus elongatus*

3.1 Introduction

The oscillation of KaiC phosphorylation patterns in the cyanobacterium *Synechococcus elongatus* is responsible for the maintenance of stable circadian rhythms in this organism [19, 22, 23]. Here we have undertaken a computational approach to understand better this complex biological network.

Mathematical models are emerging as useful tools for representing and testing our understanding of complex biological systems of a variety of scales. In particular mechanistically detailed models are being developed to capture the underlying structure, dynamics, and detailed mechanisms of biochemical networks. Such models are able to account for complex biological phenomena by representing simple kinetic relationships that are readily simulated and analyzed.

Even primitive networks of few proteins are made quite complex by the existence

of multiple modification states and complexes formed. In this study we use a mass action approach for analyzing the relationship between network topology and kinetic behavior in the *in vitro* circadian clock of the freshwater cyanobacterium, *S. elongatus*. The cyanobacterial circadian clock enables *S. elongatus* to adapt cellular performance to daily changes in the environment and provides a daily rhythm to photosynthetic regulation [16, 15]. Kondo et al. has shown that circadian oscillations can be reconstituted *in vitro* using only three proteins: KaiA, KaiB, and KaiC [31]. KaiC phsophorylation oscillates with the circadian period. Although it is known that KaiC phosphorylation oscillates with a circadian period, the fundamental mechanism and a clear understanding of the dynamics is indeterminate. Understanding such complexity may be advanced through mathematical modeling.

The cyanobacterial circadian clock is an ideal candidate to assess methodology due to the stable KaiC phosphorylation cycle *in vitro* as an expected emergent behavior of the system, which purportedly contributes to the robustness of the circadian rhythm for cyanobacteria *in vivo* [19]. Plus the abundance of experimental measurements are available for verification of mathematical models, testing assumptions and postulating predictions.

Hence, we produced a mass action model representing the circadian behavior put forward by the Rust et al. model [40]. The approach utilizes a mechanism-based chemical kinetic model to describe the network topology. Mathematical formulation of the mass action kinetics is based on sparse matrices and Kronecker products that allow efficient and straightforward application of a variety of numerical methods. In particular, we demonstrate that simulation, parameterization, sensitivity analysis, and network topology partitioning can be performed effectively within this mass action modeling framework.

In this model we have explicitly represented KaiC as switched between an unactivated or activated enzyme, where autophosphatase and autokinase are regulated by

bound KaiB or free KaiA respectively [42]. The switch-like pattern conforming to the presence of free KaiA perserves the oscillatory dynamics of the Rust et al. model. Recent work by Johnson et al. hypothesizes tha the switch-like pattern is driven by free KaiA binding to the allosteric regulation site of KaiC, resulting in a conformation change that may enhance the autophosporylation rate of KaiC [21, 24]. The conformation change may be due to KaiA disrupting the fold of the S-shaped loop by KaiA binding to the C2 domain of KaiC in a recurrent fashion during autokinase [21, 24, 23].

Chapter 4

Methods

4.1 Model Structure

We adopted the model of oscillatory phosphoform interconversion from the work of Rust et al. [40] and converted the model from Hill–Langmuir kinetics [14] to mass action kinetics. This formulation allows the model to access a variety of optimization and analysis tools available for mass action models.

Mathematically such a model is represented as a system of ordinary differential equations,

$$\dot{y}(t, p; y_0(p)) = f(y(t, p; y_0(p))) \tag{4.1}$$

$$y(0, p; y_0(p)) = y_0(p) \tag{4.2}$$

where $y(t, p; y_0(p)) \in \Re^{n_y}$ are the state variables and $p \in \Re^{n_p}$ are the parameters. We write $y_0(p)$ as an initial condition dependent on the parameterization in anticipation that this model is an intermediate limit cycle oscillator [45] and $y_0(p)$ will represent a point on the limit cycle. The full model contains 75 distinct chemical species concentrations, and 349 elementary reactions of the first- and second-order; there are no zeroth-order reactions (e.g. no protein degradation or synthesis) in this post-

translational oscillator (PTO) model. The model is parameterized with 26 unique reaction rate values and six non-zero initial concentration values. The full system is available for download as supplementary information (SI).

The model accounts for time-varying biochemical concentrations (state variables) of heteromultimeric complexes formed by the Kai proteins, along with the intermediate protein complexes, such as Michaelis complexes, within the autokinase and autophosphatase reactions of KaiC that maintain oscillation. The two main sites of KaiC that accept phosphorylation are serine 431 (S431) and threonine 432 (T432) [40, 47, 34]. Phosphorylation and dephosphorylation reactions are implemented for interconversion of four KaiC phosphoforms: unphosphorylated KaiC (U-KaiC), serine-phosphorylated KaiC (S-KaiC), threonine-phosphorylated KaiC (T-KaiC), and doubly-phosphorylated KaiC on the serine and threonine sites (D-KaiC). The outputs of interest in this study, D-KaiC (D_T), S-KaiC (S_T), T-KaiC (T_T), and U-KaiC (U_T), are defined as some linear combination of state variables formed by multiplication of the row vector c^T (Table A.11 in *SI*) with the state variables $y(t, p; y_0(p))$ as follows:

$$[D_T \;\; S_T \;\; T_T \;\; U_T]^T = c^T \cdot y(t, p; y_0(p)) \tag{4.3}$$

The model represents KaiC phosphoforms in unactivated (D,S,T,U) or KaiA-bound (D:A,S:A,T:A,U:A) state for dephosphorylation, and in activated (D*,S*,T*,U*) state for phosphorylation (Figure A-1(II) in *SI*). KaiC phosphoforms are allosterically regulated by free KaiA enhancing autophosphorylation, but in the absence of free KaiA autodephosphorylation occurs [48, 23]. The Rust et al. model dynamics were preserved by first-order kinetics representing phosphoform interconversion of KaiC independent of KaiB [40]: interconversion rates of unactivated and KaiA-bound KaiC occur at the basal effect in the absence of free KaiA (Table A.3 in *SI*), and phosphoform interconversion rates of activated KaiC occur at enhanced rates (Table A.4 in *SI*) [40]. KaiA-KaiC interactions control the switching between the KaiC phosphorylation and dephosphorylation phases [23]. During autophosphorylation, the transition

state KaiA-bound KaiC can reversibly dissociate to unactivated KaiC or irreversibly dissociate to activated KaiC (Table A.2 in *SI*) . In our model we support the hypothesis that free KaiA allosterically regulates KaiC, causing a conformational change from KaiA-bound KaiC to activated KaiC when free KaiA is at maximal effect in the system. KaiC remains unactivated when free KaiA is absent from the system (Figure 5-3).

The phosphoform interconversion has a regulatory feedback on the amount of free KaiA present in the system. The S-KaiC phosphoform has a strong affinity to form a complex with KaiA and KaiB in the C2 domain [2]. This {S|S:A|S*}:B:Ai_2 complex effectively sequesters a dimer of KaiA, inducing KaiC dephosporylation through the absence of free KaiA (Figure A-1(III.b) in *SI*). The mass action model accounts for combinatorial intermediate binding states of the KaiABC complex, where the transient KaiABC formation is represented by second-order kinetics (Table A.1 in *SI*). The assembly of KaiA and KaiB to S-KaiC is irreversible, but as this KaiABC complex modulates between KaiC phosphoforms, KaiB and sequestered KaiA disassemble from D-KaiC, T-KaiC, and U-KaiC (Figures A-1(I) and A-1(IV) in *SI*). The strong binding affinity between KaiB and S-KaiC will not disassemble unless the complex undergoes phosphoform interconversion. Note that once KaiB disassembles from D-KaiC, T-KaiC, or U-KaiC, the phosphoform interconversion to S-KaiC may occur, followed by further disassembly of sequestered KaiA from S-KaiC (Figure A-1(III.a) in *SI*). The formation of the KaiABC complex is not explicitly represented in the Rust et al. model. Instead, the concentration of free KaiA is modeled with the term

$$A = max\{0, [KaiA - 2 \cdot S]\} \tag{4.4}$$

corresponding to the instantaneous association of S-KaiC with KaiB to sequester a KaiA dimer [40].

4.2 Parameterization

Initial parameter values were obtained from the Rust et al. model for the first-order reactions where KaiC transitions between the D-KaiC, S-KaiC, T-KaiC, and U-KaiC phosphoforms (Tables A.5, A.6, A.7, and A.8 in *SI*). Our parameterization for phosphoform interconversion was initialized to the Rust et al. model parameterization except for the negative rate constants on serine dephosphorylation in the presence of free KaiA which we set to zero [40].

To represent the KaiABC formation and effects of free KaiA with elementary reactions, we replaced Equation 4.4 and the Hill-Langmuir reaction rate function in the Rust et al. model with fast kinetics. KaiABC assembly occurs on a faster timescale than KaiABC disassembly and KaiA activity, effectively accounting for the negative feedback loop in S-KaiC inhibition on KaiC autokinase [40]. The Rust et al. phosphoform interconversions occur at slower kinetics. With these initializations, model parameterization was computed in two steps: (1) to measure the best fit to the numerical integration of the Rust et al. model, and then (2) to aggregate the best fit from (1) and the best fit to the phosphorylation and dephosphorylation partial kinetics of the Rust et al. model.

Because many complexes are assumed to act with identical kinetics, the system was initialized with 26 unique reaction rate values to describe the 349 elementary reactions in the model. The initial species concentrations in both the mass action kinetic model (MA) and the Rust et al. Hill-Langmuir model (HL) were fixed to the values specified in *SI* Table A.9. Using the KroneckerBio package [5], in the first step we fit the model to that of Rust et al. from randomly generated starting points where each parameter was varied within $\pm$ three orders of magnitude. The parameter optimization on the full nonlinear system was performed using a gradient-based adjoint Lagrangian method. Least-squares fitting was used for fitting the mass action kinetic model to the Rust et al. Hill-Langmuir model. The cost function that was minimized

was the sum-of-squares error on the trajectory points of KaiC outputs (Equation 4.3),

$$\min \sum_{i=1}^{N} \left| c^T \cdot y_{MA}(t_i) - y_{HL}(t_i) \right|^2 \tag{4.5}$$

where c^T is a control row vector (Table A.11 in *SI*) that extracts the common species from the simulation. Here the parameters were bound within $[0,1.8 \times 10^{13}\ cm^3 h^{-1}]$; the lower-bound is set to be non-negative for feasible mass action kinetics in equilibria and the upper-bound is set to the rate of cell diffusion. Due to the wide range in valid parameterization, the stiff solver ode15s in MATLAB was necessary to efficiently compute the time derivatives and the Jacobian of the system for the solution of gradient-based minimization. Furthermore, the best optimum, with the lowest target function value, was accepted as the global optimum.

With the resulting parameterization from the first step in fitting the model, in the second step multiple fits were performed to simultaneously fit the mass action kinetic model to the numerical integration and the phosphorylation and dephosphorylation partial reactions of the Rust et al. model. The three experimental trajectories are fits to the SDS data presented by Rust et al. as non-oscillatory partial reactions of the phosphorylation and dephosphorylation kinetics. In order to parameterize the model to take these experimental trajectories into account, the cost function from the first fit was updated to minimize the aggregate of the target functions

$$\min \sum_{i=1}^{N} \left| c^T \cdot y_{MA}(t_i) - y_{HL}(t_i) \right|^2 + \sum_{j=1}^{3} \sum_{i=1}^{N_{expt_j}} \left| c^T \cdot y_{MA_{expt_j}}(t_i) - y_{HL_{expt_j}}(t_i) \right|^2 \tag{4.6}$$

where the first summation represents a goodness-of-fit to the Hill-Langmuir model and the second (double) summation represents a goodness-of-fit to the three experimental sets of trajectories. The original experiment trajectories are illustrated in the Rust et al. publication in the following figures: 2A, 2B (or S2), and S3 [40].

4.3 Sensitivity Analysis

To assess the oscillations of the KaiC phosphoform interconversions, we used the fitted mass action model in detailed sensitivity analysis. By probing infinitesimal variation in parameters and initial concentrations of the state variables away from the optimized model, influences on the state variable trajectories and their derived quantities were useful in understanding the biological network topology and processes setting emergent system behavior. We performed sensitivity analysis based on the oscillatory behavior of this system by determining the influence of each state variable and elementary reaction on system properties.

Because this mass action model is based on a set of chemical reactions without protein synthesis or degradation, mass conservation relationships of the KaiA, KaiB, and KaiC proteins are in equilibria (Table A.10 in *SI*). Upon inspection of the state-transition Monodromy matrix $\mathbf{M}$ defined by

$$M(p) = \left.\frac{\partial y}{\partial y_0}\right|_{T(p),p,y_0}, \text{ and} \tag{4.7}$$

$$\mathbf{M} = M(p) - I \tag{4.8}$$

we were able to determine that there are dependencies in this model on initial concentrations and parameterization. For limit cycle oscillators (LCO) there is exactly one eigenvalue of $\mathbf{M}$ on the unit circle, being full rank for a closed orbit, and for non-limit cycle oscillators (NLCO), all eigenvalues of $\mathbf{M}$ are on the unit circle, being rank deficient at zero or one for a closed orbit. The periodicity of the LCO has transient behavior (i.e. approaches the stable limit cycle from any initial concentration) and is determined solely by the parameterization of the system whereas the periodicity of NLCO has no transient behavior and is determined by both initial concentrations and parameterization of the system. Since the rank defficiency of $\mathbf{M}$ is $rank(\mathbf{M}) = 73$, this model has mathematical relations to LCOs and NLCOs in that transient behavior persists and that the periodicity is determined by both initial concentrations and

parameterization [45].

The oscillatory behavior of this model has been classified as an intermediate-type limit cycle oscillator (ILCO) according to Wilkins et al., a basis for the methods presented in our sensitivity analysis [45]. Because the parameterization influences the shape and location of the ILCO trajectory, the parametric sensitivities for the state variables initialized to the limit cycle were not set to zero, as is usually done for systems where initial concentrations are independent of the parameters. Therefore the Boundary Value Problem (BVP) is formulated for the initial concentrations $y_0(p)$ and the period of oscillation $T(p)$ on a limit cycle such that:

$$y(T(p), p; y_0(p)) - y_0(p) = 0 \tag{4.9}$$

$$m^T \cdot y(t, p; y_0(p)) = \varphi \tag{4.10}$$

where m^T is the transpose of the mass conservation relationships matrix and $\varphi = [A_T \quad B_T \quad C_T]^T$ (Table A.10 in *SI*) for $y(t, p; y_0(p))$, which is given by the solution from Equations 4.1 and 4.2.

Equation 4.10 is dictated by the rank defficiency of $\mathbf{M}$, which must be full rank to compute detailed sensitivities for the system on the limit cycle [45]. According to Wilkins et al., a total of $i = (n_y + 1 - rank(\mathbf{M})) = 3$ conditions for Equation 4.10 were required. Because the phosphoform interconversion occurs in a closed-loop PTO system, Equation 4.10 was implemented as a constraint such that the total of each KaiA, KaiB, and KaiC proteins be constant for all times t along the trajectory. By enforcing the mass conservation relationships, the mass action model was stabilized for any defined φ in the following sensitivity analysis [11].

To tease out the effects a single parmeterization may have on the system, the fitted mass action model was "unlumped" such that each of 349 elementary reactions were represented as 349 independent reactions with unique rate constants instead

of the 26 shared parameterizations utilized in the fitting. The model itself was left unchanged, but now it is possible to distinguish the effects that each parameter has on specific reactions. This method does not imply that the biological system may be controlled at such granularity, but rather serves to further isolate the processes and mechanisms that set the oscillatory behavior.

Full sensitivities of the unlumped mass action model were accurately and efficiently calculated by trapezoidal rule integration. Because there is exponential convergence of trapezoidal rule integration when computing periodic functions, the actual error in our results decay at $2 \cdot \left(\frac{2\pi}{N}\right) \cdot \left(\frac{e}{2N}\right)^N$ for partitioning the interval [0,T] into N uniform subintervals [44]. The low error is because the trapezoidal rule ensures that in those regions where the graph is concave up, the trapezoids overestimate the true area under the curve, and likewise when the trajectory is concave down thus cancelling out the errors. Due to the stepwise integrations of the trapezoidal rule formulation for calculating partial derivatives of the solution from Equations 4.1 and 4.2, $\mathbf{M}$ was computed for free in Equation A.1, which would not have occurred using a native integrator of MATLAB (Equations A.1 and A.2 in *SI*).

Intermediate partial derivatives had to be calculated in order to compute local, first-order sensitivities of the system to initial conditions, state variables, and parameterization. Due to the class of this system as an ILCO, the quantities computed for the period, phase, and amplitude sensitivities relate to well-defined derived functions for this class of oscillating dynamical systems. To capture the influence that the initial concentrations have on the period, phase, and amplitude sensitivities, the dependency of the initial concentrations on the parameterization was accounted for by solving $S(T(p), p; 0)$ which is the parametric sensitivity for zero initial conditions at time $T(p)$ and solving $S_0(p)$ which is the non-zero sensitivity to initial conditions, in order to compute the resulting parametric sensitivities dependent upon initial conditions $S(t, p; S_0(p))$.

To begin with, an intermediate partial derivative (derived from the relationship in Equation 4.9) was computed to represent parametric sensitivities of the system at time $T(p)$ with sensitivities to initial concentrations being set to zero:

$$S(T(p),p;0) = \left(\left. \frac{\partial y}{\partial p} \right|_{T(p),p;y_0(p)} \right)_{y(0)=const.} \tag{4.11}$$

Then, to uniquely determine the nonzero sensitivities of the unlumped mass action model to the initial concentrations $S_0(p)$, Equation 4.9 was differentiated with respect to the parameterization $\mathbf{p}$ and the state-transition matrix $\mathbf{M}$ was stabilized according to the mass conservation conditions in Equation 4.10, as shown in the resulting set of equations rewritten in matrix form as

$$\begin{bmatrix} \mathbf{M} & \dot{y}(T(p),p;y_0(p)) \\ m^T & 0 \end{bmatrix} \begin{bmatrix} \left. \frac{\partial y_0}{\partial p} \right|_p \\ \left. \frac{\partial T}{\partial p} \right|_p \end{bmatrix} = - \begin{bmatrix} SP \\ m^T \end{bmatrix}. \tag{4.12}$$

The inclusion of mass conservation relationships (m^T) made $\mathbf{M}$ full rank so that we could solve the system of equations for the matrix of unknowns

$$\begin{bmatrix} \left. \frac{\partial y_0}{\partial p} \right|_p \\ \left. \frac{\partial T}{\partial p} \right|_p \end{bmatrix} \tag{4.13}$$

was then solved for $S_0(p)$ along with the period sensitivities computed for the solution at time $T(p)$. With meaningful sensitivities now captured in terms of parameterization and initial concentrations as $S(t,p;S_0(p))$, phase and amplitude sensitivities were also computed (Equations A.3, A.4, A.5, A.6, A.7, and A.8 in *SI*) [45].

Chapter 5

Results and Discussion

The circadian oscillations of KaiC phosphorylation is a well-observed phenomena of this biochemical network. The autophosphatase and autokinase activities [32, 46] of the KaiC enzyme [28] are modeled here, exhibiting oscillatory phosphoform interconversion at serine 431 (S431) and threonine 432 (T432) sites [34, 47] in the C2 domain [34, 33, 47]. Rust et al. suggest that KaiC autophosphorylates and autodephosphorylates in an ordered pattern where free KaiA enhances autophosphorylation and the presence of KaiB complexed with S-KaiC sequesters free KaiA and thus diminishes the effect of KaiA on KaiC [29, 33, 40].

To further explore this interpretation, we converted the model of Rust et al. [40] for the circadian clock of *Synechococcus elongates* to a mass action kinetic model, which enabled us to apply a collection of modeling and analysis tools that we have developed around mass action modeling. The original Rust et al. model was built and parameterized using experimental data for protein phosphorylation and dephosphorylation. We fit our model to trajectories directly computed from their model, to achieve model equivalence over the range of experimental conditions used in the original fit.

Figure 5-1A shows an overlay of oscillatory trajectories for the various KaiC phosphoforms between the original Rust et al. model and our mass action version. The

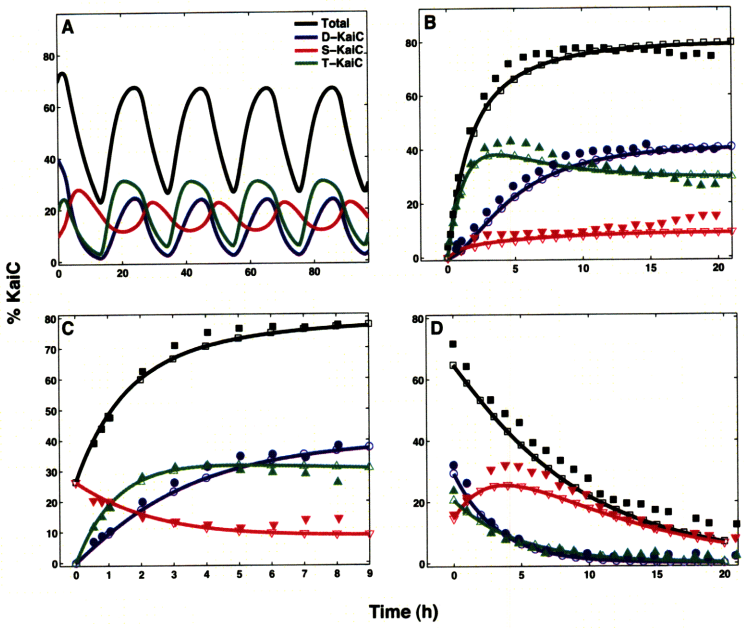

Figure 5-1: **Model Verification.** Mass action modeling dynamics overlayed with the original Rust et al. dynamics. (A) The original Hill-Langmuir model and our mass action model trajectories overlaid. Total KaiC accounts for the total amount of phosphorylated KaiC, excluding U-KaiC (unphosphorylated): D-KaiC (doubly phosphorylated on serine 431 and threonine 432), S-KaiC (serine 431 phosphorylated), and T-KaiC (threonine 432 phosphorylated). Experimental data (solid symbols) for phosphorylation (B-C) and dephosphorylation (D) kinetics was used by Rust et al. to fit their model (hollow symbols).

trajectories overlay so closely as to be indistinguishable in the figure, which indicates that reinterpretation of the original model in mass action terms did not alter its behavior with respect to the fitting conditions. The model functions as a limit cycle oscillator with a free-running period of approximately 21 hours, and the initial conditions of the Rust et al. model are somewhat off the limit cycle, as can be seen from the differences in heights between the first peak and the rest for each of the species. Figures 5-1B, 5-1C, and 5-1D show a similar overlay of the trajectories developed here and those from Rust et al. (hollow symbols), together with the experimental data (solid symbols) collected by Rust et al. that was used to fit their model.

The experimental data for Figures 5-1B and 5-1C resulted from SDS-PAGE experiments in which the abundance of each KaiC phosphoform was measured after treat-

ment with KaiA for various time periods starting from different initial states (Table A.9 in *SI*). Dephosphorylation was prevented by the absence of KaiB. The experimental data in Figure 5-1D is from dephosphorylation experiments in the presence of KaiB and the absence of KaiA.

Together the results show essentially perfect quantitative agreement between the original Hill-Langmuir model and the new mass action model of this system over the range of conditions used to parameterize the original model. Thus, we will use the mass action model in what follows, so that we can apply tools we have developed specifically for this class of kinetic representations.

The mass action model consists of 75 distinct chemical species concentrations, 26 unique reaction rate values, and six non-zero initial concentration values. However, throughout the presentation of the results for the full system, we focus on an abstracted visual representation that includes only the 13 species that accrue to significant concentrations. Intermediate protein complexes, such as Michaelis complexes, account for over 60% of the species represented. The majority of intermediate complexes and a number of other species exist in inappreciable amounts, thus permitting the abstracted representation focusing on just 13 major species.

Figure 5-2 shows an abstracted visual representation and illustrates relative reaction rates (Figure A-1(I) in *SI* for the full model). The arrow thicknesses represent reaction rates, which are weighted logarithmically according to magnitude, with the thickest arrows representing the fastest kinetics. The reaction rates along the planes for phosphoform interconversion are equivalent in the mass action model and the Rust et al. model (Figure A-1(II) in *SI*). Allosteric regulation of KaiC by free KaiA runs perpendicular to these planes, and the combinatorial intermediate binding states in the assembly and disassembly kinetics of the KaiABC complex are noticeably collapsed in this abstraction (Figure A-1(III) and A-1(IV) in *SI*).

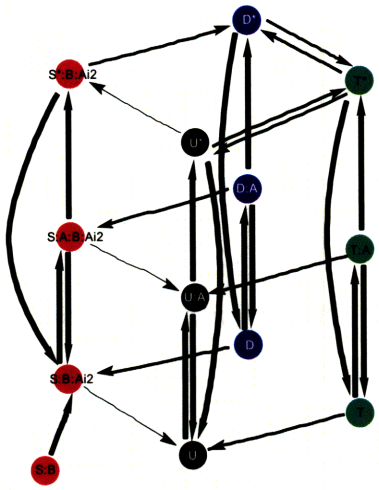

Figure 5-2: **Abstracted Visual Representation of the Mass Action Model.** Here is an abstraction of our mass action model where arrow thicknesses represent reaction rates that are weighted logarithmically according to magnitude where the thickest arrows represent the fastest kinetics. The reaction rates are approximately: ≥ 1 (thick arrow), ≥ 0.1 (medium arrow), < 0.1 (thin arrow).

The time course of these appreciable KaiC complexes, free KaiA, and free KaiB are plotted in Figure 5-3. We identify two regimes (Phase I and Phase II) of Kai protein behavior within the circadian period. Phase I is characterized by the absence of free KaiA, progressive dephosphorylation of KaiC species, and saturation of the S-KaiC:KaiB with sequestered KaiA. Phase II is characterized by the appearance of activated KaiC species (D*,S*,T*,U*), the presence of free KaiA, and a preponderance of phosphorylation kinetics. During dephosphorylation, essentially only the lower plane of Figure 5-2 is populated because free KaiA is necessary to activate KaiC species to the middle (Michaelis complex) and upper planes. In the lower plane, unactivated KaiC species can only dephosphorylate. Phase II populates the entire figure and drives the oscillatory dynamics in a manner that can be tracked but isn't readily understood. Further analysis of the model is necessary to reveal relationships between network structure and oscillatory dynamics.

Figure 5-4 shows the sensitivities of the oscillatory period with respect to the relative rate parameters of the model. The arrow thicknesses represent scaled period sensitivities that are weighted logarithmically according to the highest magnitude,

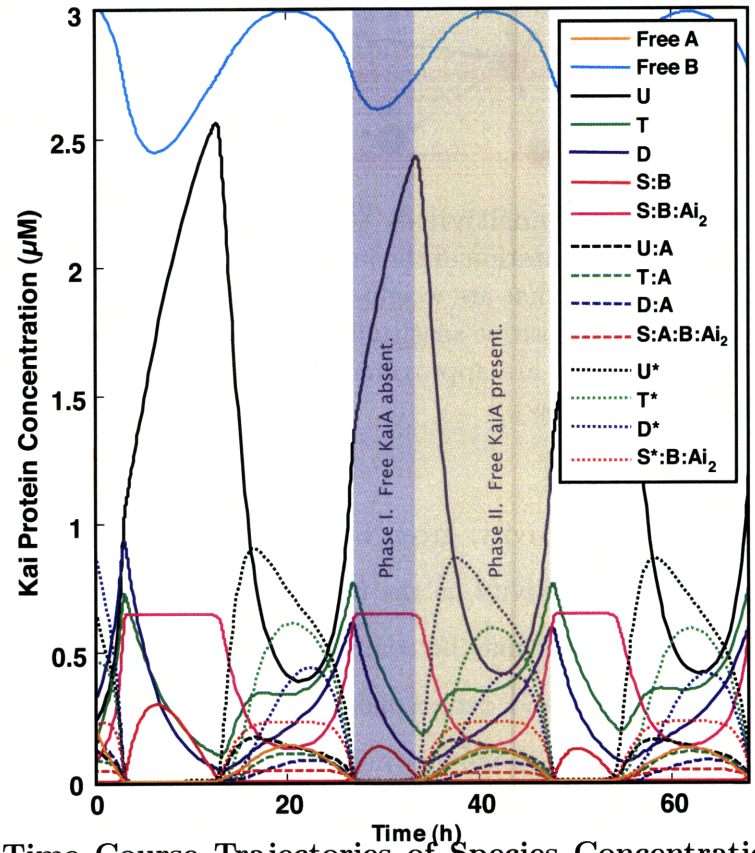

Figure 5-3: **Time Course Trajectories of Species Concentrations.** Here we plot the trajectories of the species (state variables) that occur at appreciable concentrations. The presence or absence of free KaiA in the model drives two regimes of behavior, Phase I and Phase II, within the circadian period. During autokinase (Phase II), unactivated S-KaiC binds to KaiB and sequesters free KaiA to form the KaiABC complex, as shown by the magenta trajectory. Furthermore, all free KaiA in the system is sequestered during autophosphatase (Phase I).

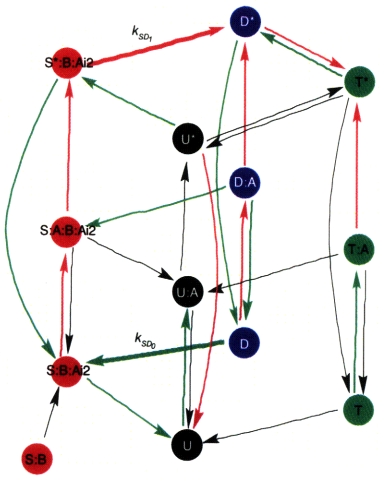

Figure 5-4: **Scaled Period Sensitivities** $\frac{\partial \log T}{\partial \log p}$**.** Period sensitivities are imposed on this abstracted visual representation of the mass action model. The arrow thicknesses represent period sensitivities that are weighted logarithmically according to the highest magnitude where red is positive sensitivity and green is negative sensitivity. The period sensitivity magnitudes are approximately: ≥ 1 (thick arrow), ≥ 0.1 (medium arrow), < 0.1 (thin black arrow).

with red being positive sensitivity, green being negative and black being close to zero. The positive (red) sensitivity on the reaction rate k_{sd}^1 has a dominant lengthening effect on the period that may be compensated by the shortening effect due to k_{ds}^0. These phosphorylation and dephosphorylation dynamics between S-KaiC and D-KaiC play a significant role in modulating the period. The allosteric regulation of free KaiA supports the self-consistent processes that phosphorylated KaiC (excluding T-KaiC) activation slows the circadian period and phosphorylated KaiC inactivation speeds the circadian period. The reverse behavior occurs for unphosphorylated KaiC as shown in Figure 5-4.

To understand better the system behavior between the two phases, we partitioned the circadian period into a dephosphorylation interval (Phase I) and a phosphorylation interval (Phase II) as shown in Figure 5-5. According to our initial observations from Figure 5-3, we tracked species concentrations separately during these two regimes. To track species concentrations in a given interval, partitioning of the species was accomplished by enzyme-driven switch-like behavior. During the dephosphorylation

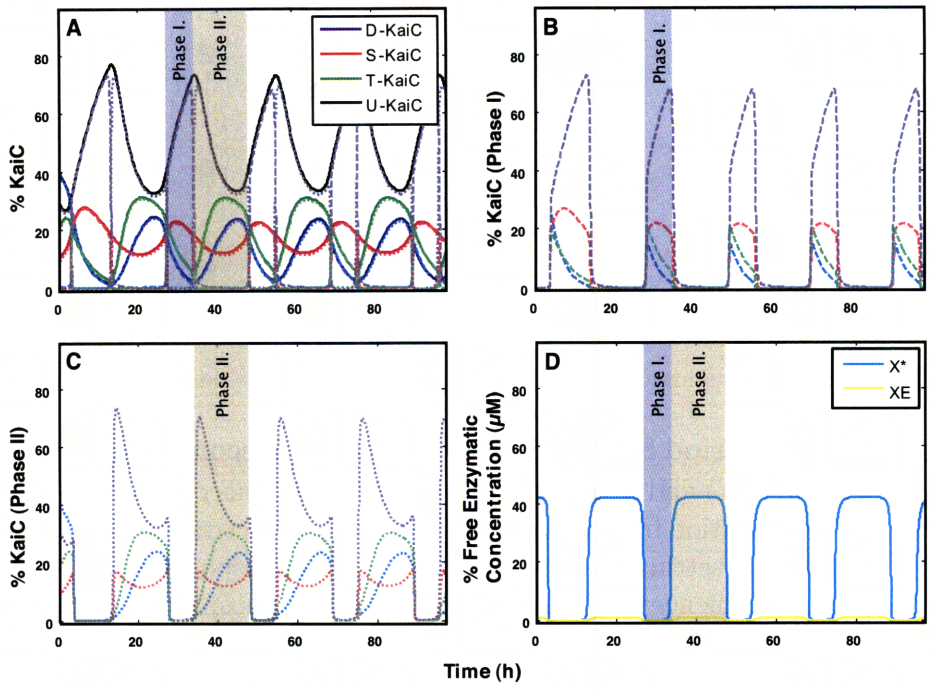

Figure 5-5: **Circadian Period Decomposition.** The mass action model was decomposed into a dephosphorylation interval (B) and a phosphorylation interval (C) by implementing enzyme-driven switch-like behavior (D). (A) The superimposition of Phases I (B) and II (C) results in the full trajectories of the mass action model.

interval, the switch was in 'off' mode due to the absence of free KaiA; likewise during the phosphorylation interval, the switch was in the 'on' mode due to the presence of free KaiA.

In order to track KaiC autokinase and autophosphatase, we created an artificial species which was activated by KaiA and would bind and track KaiC behavior. Since free KaiA exists at a much lower concentration than the amount of artificial species required to complex with KaiC ($\text{KaiA}_{Total} \ll \text{KaiC}_{Total}$), an enzyme cascade was implemented as a rapid two-step process: (1) continual activation of a low concentration enzyme XE, where $\text{XE} \ll \text{KaiA}_{Total}$, which then (2) activated a high concentration species X* , where $\text{X}^* \gg \text{KaiC}_{Total}$, to rapidly and repeatedly complex with all KaiC phosphoforms. This enzyme cascade persisted exclusively during the 'on' mode; consequently X* would remain uncomplexed to KaiC once free KaiA depleted and the dephosphorylation interval initiated. As a result, all KaiC complexes in Phase II were

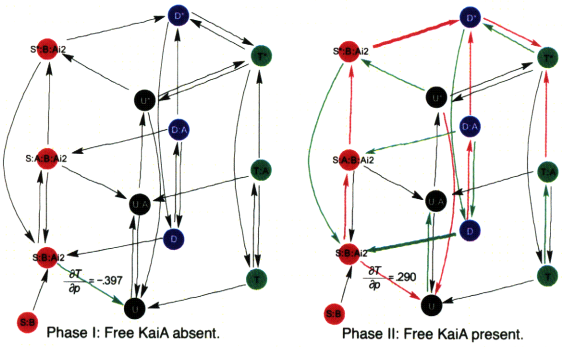

Figure 5-6: **Scaled Period Sensitivities $\frac{\partial \log T}{\partial \log p}$ for the Decomposed Period.** The dephosphorylation (left) and phosphorylation (right) intervals of a circadian period is shown here. The transition from unactivated S-KaiC to unactivated U-KaiC plays the most significant role in setting the period during KaiC dephosphorylation. Conversely, an array of kinetics influence the periodicity during KaiC phosphorylation. The arrow thicknesses and colors represent period sensitivities that are weighted logarithmically according to the same spread for period sensitivities in Figure 5-4.

bound to X* and thus differentiable in a computational experiment sense from KaiC complexes in Phase I, which were not bound to this enzyme. Through the implementation of this enzyme cascade, we were able to track transients of the system (for implementation see Tables A.12 and A.13 in *SI*).

Perturbation analysis of the *in vitro* circadian oscillator for *S. elongatus* has shown that modulations of KaiC autokinase and autophosphatase kinetics have had the most dramatic effects on period setting [29]. By performing period sensitivity analysis on each dephosphorylation interval (Phase I) and phosphorylation interval (Phase II) we were able to decompose the influence that free KaiA allosteric regulation has on KaiC phosphoform interconversion. The transition of unactivated S-KaiC to U-KaiC was determined to be a triggering process during dephosphorylation for setting the period. As shown in Figure 5-6 (left), this autophosphatase process has an overall shortening effect on the period, being the singular influence particularly when free KaiA is absent from the system. Although this same transition has the reverse effect on the period in the presence of KaiA, there are also other kinetics at play according to the heavily weighted sensitivities in the diagram. Upon closer inspection of Figure

5-6 (right), the decomposed period sensitivities during the phosphorylation interval (Phase II) are comparable in magnitude and effect to the computed full period sensitivities in Figure 5-4.

Analyzing the flux pathways for a circadian period provides further insight into dominant processes within the model. As shown in Figures 5-7A and 5-7C, the notion that the flux during the phosphorylation interval is comparable to the overall period flux is in agreement with our full period sensitivity results, indicating that the processes in the presence of free KaiA are dominant in setting a faster or slower circadian clock. A more intuitive interpretation of this figure is that activity during the dephosphorylation interval occurs mainly on KaiC in the unactivated state (Figure 5-7B), due to the fact that all activated KaiC has autodephosphorylated due to the absence of free KaiA in the system.

Yet counterintuitive to our earlier results is that a majority of the system flux distribution is through a process with relatively negligible period sensitivity (Figure 5-4), from activated U-KaiC to T-KaiC; this flux then splits to where half cycles back to activated U-KaiC and the remainder becomes phosphorylated at the serine site 5-7A. According to Rust et al. observations the sequence of phosphoform interconversion goes along the activated U-KaiC to T-KaiC, then activated T-KaiC to D-KaiC pathway. On the contrary, our flux analysis determines that near equivalent amounts of activated T-KaiC and S-KaiC are converted into the doubly phosphorylated form 5-7A. Other phosphoform interconversions leading to significant fluxes are along the processes with higher period sensitivities, although not all are accounted for.

Supplemental analysis on the scaled peak-to-peak phase sensitivities, and scaled absolute and relative amplitude sensitivities for the full period is uniform in denoting processes of interest. When comparing sequential peaks of KaiC phosphoforms, particularly the T-KaiC to D-KaiC phase sensitivities appear to have a significant influence on the ordered phosphorylation timing circuitry. In Figure 5-8B for the T-

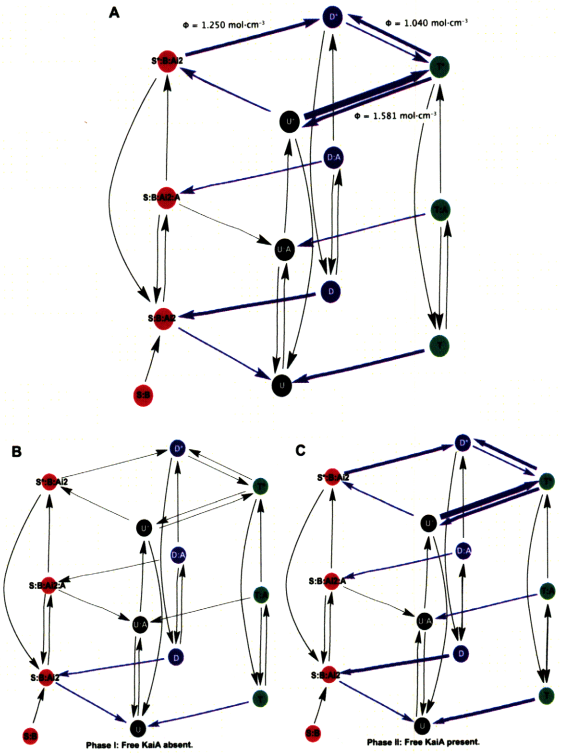

Figure 5-7: **Flux Pathways for the Phosphoform Interconversion during the Full and Decomposed Period.** The phosphoform flux distribution is shown here for a full period along with the flux distribution for the desphosphorylation interval (bottom, left) and phosphorylation interval (bottom, right) for the same period. The majority of the flux distribution occurs during the phosphorylation interval, specifically from activated U-KaiC to activated T-KaiC. The arrow thicknesses represent the overall flux for each time course according to the highest magnitude, where the magnitudes are approximately: ≥ 4 (thick blue arrow), $4 > \Phi \geq 1$ (medium blue arrow), ≥ 0.1 (thin blue arrow), < 0.1 (thin black arrow). Not graphed here are the fluxes orthogonal to the phosphoform interconversion planes, on account of these reaction rates being invariably parameterized on a faster time-scale.

KaiC to D-KaiC phase sensitivities, the phosphorylation pathway—along the initial accumulation of activated U-KaiC, followed by activated S-KaiC then to activated D-KaiC which is subsequently hypophosphorylated—includes the kinetics of discernible interest to the period sensitivities (Figure 5-4). These kinetics appear to agree in magnitude and sign; processes that are responsible for lengthening the period are also the same processes that proportionately lengthen the T-KaiC to D-KaiC time interval relative to the overall period modulation.

The amplitude sensitivities also denote particular kinetics along this same pathway that are of importance; furthermore, processes that have a lengthening effect on the period generally increase the absolute amplitude of KaiC phosphoforms (Figures A-2A, A-2C, A-2E, and A-2G, in *SI*). Notice in these figures that the activated S-KaiC to activated D-KaiC process, which is also a major lever in lengthening the period and peak-to-peak phase, accordingly results in higher amplitude oscillations. When analyzing the T-KaiC to D-KaiC phase sensitivities in Figure 5-8B and the D-KaiC absolute and relative amplitude sensitivities of Figures A-2A and 5-8B in the *SI*, a self-consistent process is that this pathway modulates the phosphoform interconversion oscillations to either a lengthened time interval with higher phosphoform peaks, or a shortened time interval with lower phosphoform peaks. The S-KaiC absolute amplitudes are affected in a similar mode along the same pathway (Figure A-2C in *SI*).

To determine the important pathways within the network, we implemented an algorithm to minimalize the full mass action network without losing oscillations. Our algorithm searched for potential subnetwork motifs that could exist where the Michaelis complex between unactivated to activated KaiC did not undergo phosphorylation or dephosphorylation but only transitioned between the unactivated and activated KaiC forms. Therefore phosphoform interconversion was only considered for unactivated and activated KaiC forms, and provided that the phosphoform interconversions of KaiC occur at equivalent reaction rates for unactivated KaiC and KaiA-bound KaiC,

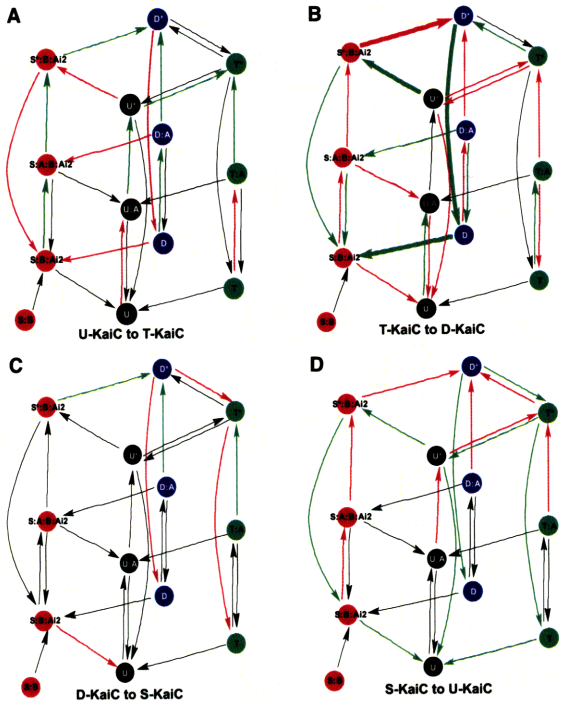

Figure 5-8: **Scaled Angular Peak-to-Peak Phase Sensitivities $\frac{\partial \gamma}{\partial p}$.** The phase sensitivities are weighted logarithmically according to the same spread for period sensitivities in Figure 5-4. The peak-to-peak analysis was computed for sequential peaks starting from in between the dephosphorylation and phosphorylation intervals of the period, when U-KaiC is at a maximum. These phase sensitivities are diametric depending on which peak is ordered first, such that the D-KaiC to T-KaiC phase sensitivities has the same magnitude as the T-KaiC to D-KaiC phase sensitivities but with an opposite sign.

the complexity of searching for an oscillating minimalized model was decreased manifold. Our approach took into account all the combinatorics of unactivated KaiC phosphoform interconversion, activated KaiC phosphoform interconversion, and KaiA allosteric regulation that would conserve mass. Based on our understanding of the known molecular mechanisms, no acyclic network motifs were allowed and a network with atleast one cycle was enforced to account for the feedback loop to drive oscillatory behavior.

From our analysis we found a collection of minimalized networks that maintained oscillations; the two most minimalized networks are shown in Figure 5-9. Both of these minimalized networks include processes discussed in our results for the decomposed period, the overall sensitivity analyses, and the flux pathways. Consistent to our prior results and to the Rust et al. publication is the process in the minimal networks denoting the ordered hypophosphorylation from activated to unactivated D-KaiC, followed by threonine dephosphorylation to unactivated S-KaiC, and completing the dephosphorylation cycle with the accumulation of unactivated U-KaiC. The core phosphorylation cycle may be interpreted to have much more variation in dynamics as denoted by the discrepancies in ordered phosphoform interconversion, as shown in Figures 5-9A and 5-9C. The phosphorylation cycle in Figures 5-9A and 5-9B is well-described in the Rust et al. interpretation: "Starting from the unphosphorylated state, KaiA promotes phosphorylation that is kinetically favored at T432; subsequent phosphorylation at S431 produces ST-KaiC" [40]. The alternative phosphorylation dynamics in Figures 5-9C and 5-9D depict other core processes ancillary to the kinetically favored phosphorylation to produce T-KaiC, as noted by Rust et al.

Our second minimalized model (Figures 5-9C and 5-9D) discerns an important role that T-KaiC plays which is not addressed by the original study. ST-KaiC can amass from threonine phosphorylation on S-KaiC or serine phosphorylation on T-KaiC, but the kinetic favorability of U-KaiC to be phosphorylated on the threonine site conducts a reservoir. The accumulation of T-KaiC leads to the triggering mechanisms

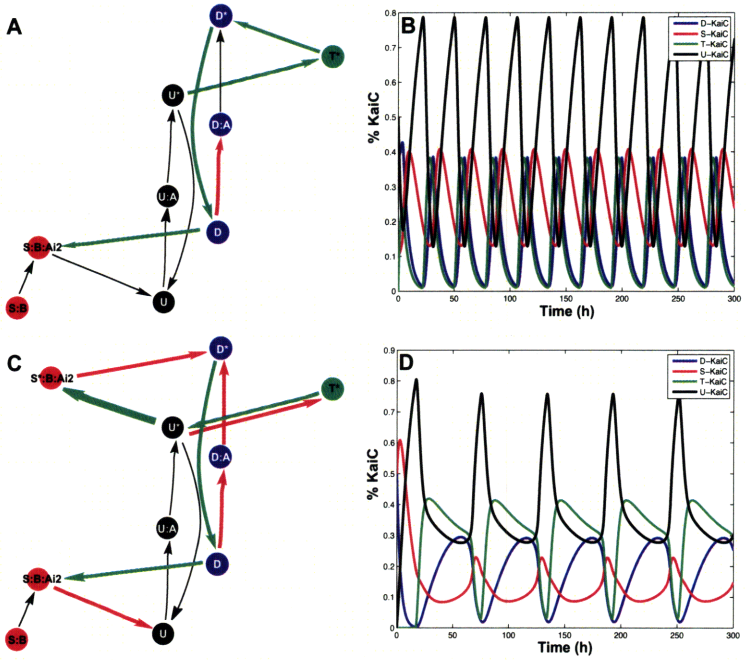

Figure 5-9: **Minimal Oscillating Networks.** A collection of minimalized oscillating networks from the original mass action model were discovered. In (A) and (C) we illustrate the two most minimalized networks we found, with the corresponding oscillatory dynamics shown in (B) and (D) respectively. These diagrams show distinct sequences of phosphoform interconversion. The arrow thicknesses and colors in (A) and (C) represent period sensitivities that are weighted logarithmically according to the same spread for period sensitivities in Figure 5-4.

between the phosphorylation and dephosphorylation phases by further modulating the quantity of available S-KaiC to sequester free KaiA. In our most minimalized networks, the transition from U* to T* was necessary to maintain oscillations, and is also the same process in the full mass action model through which the majority of the system flux distribution flows.

Our model supports recent experimental data revealing a self-sustaining sequential process of phosphoform interconversion in setting the circadian clock [33, 40] . In attempt to understand this notion further we apply mass action modeling and analysis techniques to tease out molecular mechanisms of the underlying timing circuit. We demonstrate that there are levers within the dephosphorylation and phosphorylation

phases which significantly contribute to the oscillatory dynamics of the *S. elongatus* circadian clock, namely that (1) the transition from unactivated S-KaiC to U-KaiC directly influences the frequency of the period by setting the duration of the dephosphorylation phase, that (2) the dynamics from activated S-KaiC to D-KaiC and from unactivated D-KaiC to S-KaiC respectively counterbalance positive and negative effects on the periodicity, and that (3) the S-KaiC sequestration of free KaiA is not the only significant pooling mechanism in the system. Initially the accumulation of activated T-KaiC is kinetically favored over the accumulation of activated S-KaiC, leading to a reservoir of T-KaiC. Because the flux from activated S-KaiC and activated T-KaiC to D-KaiC are equivalent to each other, both these phosphorylation sequences are significant to the phosphorylation cycle. That is, where S-KaiC pools due to the sequestration of free KaiA, activated T-KaiC has a compensatory effect in that process by gradually releasing into activated U-KaiC or D-KaiC, which ultimately results in a controlled triggering of available S-KaiC to fully sequester free KaiA in the system, and consequently switching from the phosphorylation to the dephosphorylation interval of the period.

Chapter 6

Conclusions and Recommendations

6.1 Summary of Findings

The computational methods in this research was an integration of approaches based in law of mass action, Kronecker product, and mathematical theory. This research demonstrated the integration of experimental data and theoretical models, molecular characterization of functional activity, and subsystem identification within system behavior. The *S. elongatus* circadian clock was a preferable model because the analysis of feedback mechanisms in biological systems is challenging in that it cannot be understood through conventional data analysis, data mining, or machine learning because dynamic systems theory is required. Feedback mechanisms, as observed in the circadian clock are essential for all forms of regulation, control, and coordination at all levels of the life sciences [6].

6.2 Policy Issues

Current knowledge in systems biology is not cohesive and standardized since genes, proteins, biological systems and their associated patents have been treated as strategic knowledge-based assets [3]. The effectiveness of knowledge generated is hindered by the reality that knowledge is valued as a good and therefore bartered with the transactional costs of generating that knowledge kept in mind. This mode increases

commercialization and scientific competition between labs, creating accessibility and collaboration difficulties [36]. Arguably, the widespread dissemination of current results is necessary to validate knowledge before progressing further downstream into expensive and regulated research endeavors.

Capital costs associated with validation of systems biology predictions via 'wet lab' biology are sufficiently high. Therefore, the high costs associated with generating initial data, and the corresponding value associated with such data, has created a market for such inputs to increase downstream competition. Patent rights on these inputs have been licensed exclusively in the past; this legislation has been contentious by not addressing the potential that exclusive rights have to block marketability of products downstream. The further investment for development and commercialization of a particular input is currently fostered by Intellectual Property Rights (IPRs) on upstream research. This legislation has incited the formation of small firms who market these inputs to large firms.

Thus industry players are incentivized to accumulate an abundance of patents on chemical compounds for the purpose of recouping the large costs associated in applicable commercialization, such as preclinical and clinical trials. Even for research that is not patented, upstream players have leveraged control over data and tool dissemination through 'exact reach-through royalties' by forcing the large firms to negotiate with university and small firm proprietary claims on these inputs [36]. According to Ronald Coase, this trend away from vertically integrated firms has increased transaction costs substantially and dampened innovation by enticing firms that are downstream in biotechnology research and development to avoid research areas where there are 'patent thickets' and thus potentially large payouts to those upstream.

Therefore these considerations make lab collaboration and public-private alliances inefficient. Furthermore, there is a misalignment of stakeholder motivations and resources for players who are upstream and downstream in the biotechnology research

and development. While academia is usually more flexible in taking long-term strategic positions, large firms are forced to focus on short-term tactical positions in order to deliver products for stakeholder appraisal. Whereas large firms have resources to platform technologies and interdisciplinary teams, academia has difficulties in leveraging long-term strategic positions; there is a lack of these resources internally due to unshared investments of departments and interdepartmental competition. Amid these extremes are start-ups, which heavily rely on securing upstream patents (or exclusive licensing to upstream academia patents) in order to attract venture capitalists and secure revenues when licensing to large firms [36].

An open and collaborative model would be ideal for rapid knowledge dissemination and reduction of duplicative effort. However such public endeavors undermine the ability of businesses to form around highly interdisciplinary processes. Even though collaborative projects in systems biology have the potential to be superior in allocating human creativity, and filtering and aggregating information in comparison to the market, the low cost to contributors upstream does not offset the necessity for industry players to patent rights on marketable molecular compounds and to make the channeling of upstream knowledge gains proprietary [36]. Due to the hierarchal nature of biological information in a system, systems biology knowledge generation and dissemination are hindered by patents that exist at each of these hierarchies [3].

6.3 Policymaking

In general, policymaking comes down to funding and support [1]. However, the ethical, legal, and social implications of such policies have lasting effects in addressing bioethical questions ranging from privacy concerns to the commercialization of life. A major concern of systems biology is whether *in silico* results will always require 'wet lab' experimental confirmation, or whether the knowledge generated will have the same legal status as *in vitro* and *in vivo* tests. Political and economical advantages in circumventing preclinical trials such as 'wet lab' experiments and animal testing

has been anticipated as one of the significant contributions of systems biology in addressing societal concerns with drug testing [35]. Knowledge assessment is crucial to policymaking in addressing scientific challenges within systems biology to identify drug candidates that would have a low risk of failure when entering preclinical and clinical testing. The capability for systems biology to produce usable inputs, alleviate transaction cost and secrecy problems, and persuade industry and academia collaboration in promising lines of research are key concerns in current systems biology policymaking.

Stakeholders have argued that systems biology will push patenting and commercialization further away from biological material and more towards information. This evolution may transform biological patenting into a less litigious activity by patenting the representations of biological entities instead of the entities themselves. This shift in patenting trends may mitigate concerns raised about the private ownership of life [35]. Currently there have been few successful patents with many pending, where most of the patents are for computer tools to make predictions and effective interventions. For Technology Transfer Offices (TTOs) in university settings, software does not generally merit the cost of patent filing because, economically, software yields little in licensing revenues [36]. Yet, computer-generated models have similarities to computer software in that patenting can lead to monopolization and network externalities, such as standardization [35]. Historically, IPR in the sciences has led to monetization from downstream research in stacking licenses and blocking patents on upstream research, mainly due to the legal procedures set forth by *the Bayh-Dole Act of 1980*; therefore it has been difficult for proponents of systems biology to convince universities to disavow property rights and pursue collaborative projects [36].

For systems biology, Heller and Eisenberg's 'tragedy of the anticommons' is exacerbated because the discipline may require greater cooperation and collaboration as the dominating strategy during its formative period [3]. Therefore, to avoid competition and costly investments, collaboration endorsements have been made in the

past: National Institute of General Medical Sciences (NIGMS) Studies, specifically the Alliance for Cellular Signaling (AFCS) Study, and the World Technology Evaluation Center (WTEC) Study. In the NIGMS Study, all participants agreed to disavow IPR, which is contrary to trends in patenting since the enactment of Bayh-Dole [36]. Due to historical evidence of peer-reviewer biases and incentives to tradeoff publication credibility, the NIGMS Study instead encouraged public internet access to results in attempt to induce further collaboration beyond the scope of the Study. The AFCS Study and WTEC Study did not necessarily confirm that collaborations contribute to the "efficient integration of knowledge into the development of products and the efficient utilization of knowledge" [3]. The link between systems biology knowledge and the knowledge requirements for effective biological advancements for societal welfare is not yet well established.

6.4 Policy Recommendations

Policymakers must not look to the science to definitively resolve political debates because interpretations and metaphors matter here [39, 38]. The dissension in interpretation of experimental data and defining systems biology in terms of mechanistic models singularly misleads policymakers to believe that this science is more fixed than it actually is. The potential of biological systems is not determined absolutely, but rather relationally, and centralizing innovation on biomolecular identification is the source of much IPR litigation and in essence is "limited, limiting, and misleading" the focus and investment in scientific progression [38]. Assessment of the science for policy action is not solely dependent on the scientific results but rather on the contingency of these results to related societal and political economic outcomes of net worth [39].

Political decisions that involve a diversity of interest groups are inherently difficult to make since any adopted policy is bound to infringe on stakeholder interests. Here systems biology is thwarted as a battleground for powerful economic and political

interests due to the high stakes associated with alternative policy outcomes [39]. The politicization of science is integral to advocacy; yet scientists, clinicians, and bioethicists alike are the accountable players for employing expertise in support of positions. Lawyers, regulators, and those with commercial interests have the opportunity to manipulate 'facts' and call upon expert opinion that mutually reinforces interests of those in agreement. Incidentally this situation occurs more often than not when scientists believe that the scientific results alone provide a sufficient basis for decision-making [39]. In effect, all parties involved tend to prevent pure scientific contribution to effective policymaking, thus compromising practices in systems biology as a potential outcome.

Is the happenstance here to "make policy more scientific or the science more political" [39]? Assumptions affect both ongoing research and interpretation of research results. Therefore, the scientific community must address the aforementioned claims of systems biology and their significance for policy. Due to degrees of uncertainty and interpretations of scientific results, enactment of a particular policy may involve less science and more stakeholder justification for covert and vested interests. Even if there were to be impartiality in the actual policymaking, science in itself is arguably not a primitive truth; in the words of chemist Henry Bauer, science is "a mosaic of the beliefs of many little scientific groups" [39]. Arbitration in policymaking is unavoidable and intrinsic to how scientific endeavors are supported and funded.

Politics and pragmatism come into play especially under conditions of scientific and moral uncertainty. Debate over scientific issues increasingly relies on personal incentives, criticizing processes (i.e. peer review, sources of funding), and deligitimation of systems biology through demagoguery of the science as a matter of scientific and societal perspectives [20]. Scientific policymaking becomes less about the science and more about waging political battles through science [39]. The legitimation of systems biology usually comes by way of bargaining, negotiation, and compromise which are all political maneuverings surpassing the scope of the science itself [20].

Amidst the bureaucracy, validation of accuracy and applicability of systems biology may nonetheless be endorsed by policymaking. Consideration of scientific, clinical, ethical and political issues in an integral manner may rule out actions of false dichotomy amongst stakeholders [38]. The risk of policy enactment may be as great as the risk of no policy considerations; however, the deliberation of policymaking in of itself is prospect for consideration of questions about decision-making regarding uncertainties with systems biology, and whether those uncertainties be of scientific, clinical, moral, or political basis.

Policymaking for systems biology should explore radical shifts in power and control, in tandem with the development of the underlying theory and technology. Authoritative and non-partisan bodies should assume more responsibility in assessing scientific research and placing significance of this work into a policy context [39]. The depth and scope of challenges with systems biology is just as complex as the biological systems that are being studied. Because there are significant barriers to progress due to socioethical engagement with commercialization, it may be opportune to take an adaptive approach to policymaking for systems biology [35]. Practicing continuous and responsive improvement with short-term gains on long-term positions would proactively guide systems biology development, especially in this formative period and in anticipation of a more mature systems biology.

Appendix A

Supplemental Information (SI)

I

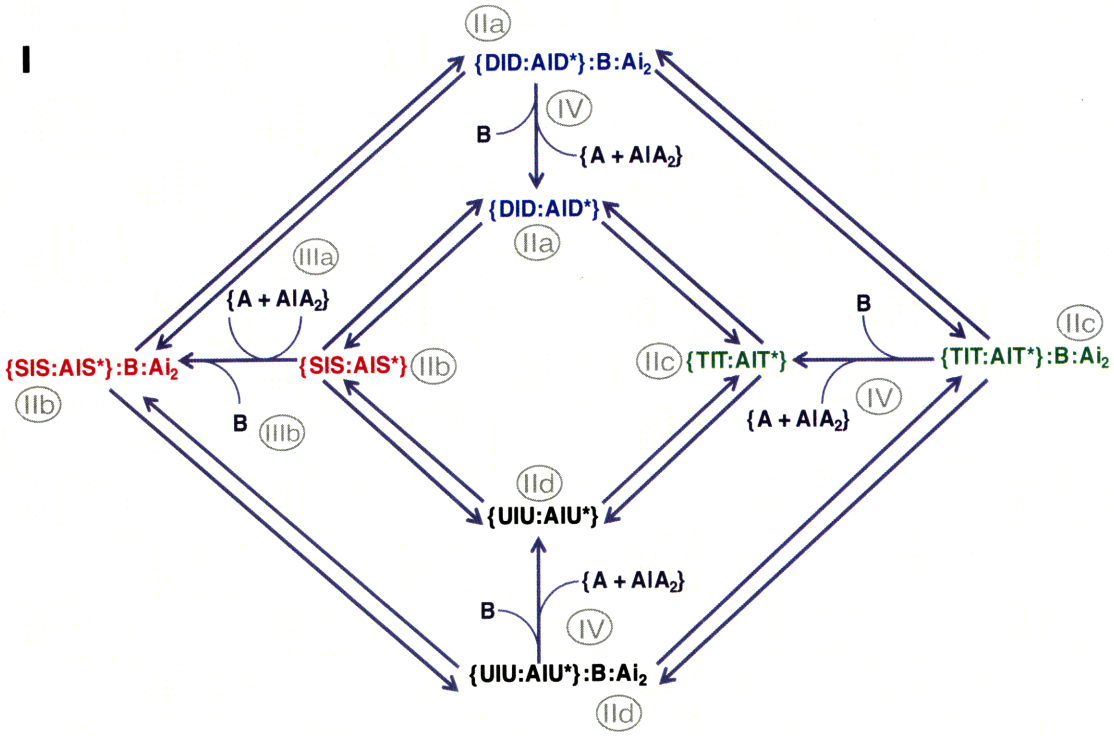
IIa
{DID:AID*}:B:Ai2
IV
B
{A + AIA2}
{DID:AID*}
IIa
IIIa
{A + AIA2}
{SIS:AIS*}:B:Ai2
IIb
{SIS:AIS*}
IIb
IIc
{TIT:AIT*}
B
IIc
{TIT:AIT*}:B:Ai2
B
IIIb
{A + AIA2}
IV
IId
{UIU:AIU*}
{A + AIA2}
B
IV
{UIU:AIU*}:B:Ai2
IId

II

a

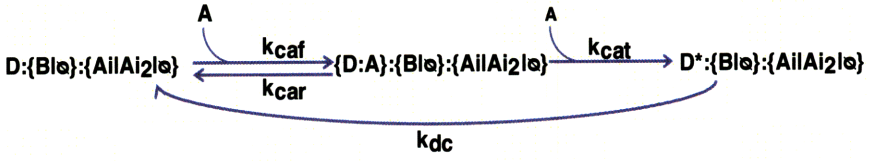
A
kcaf
D:{Blo}:{AilAi2lo}
{D:A}:{Blo}:{AilAi2lo}
A
kcat
D*:{Blo}:{AilAi2lo}
kcar
kdc

b

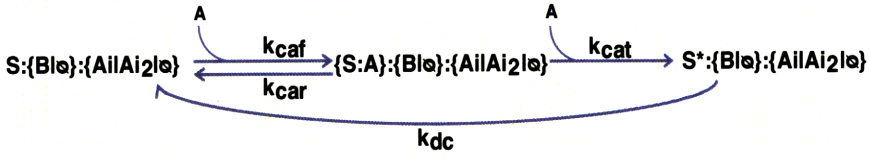
A
kcaf
S:{Blo}:{AilAi2lo}
{S:A}:{Blo}:{AilAi2lo}
A
kcat
S*:{Blo}:{AilAi2lo}
kcar
kdc

c

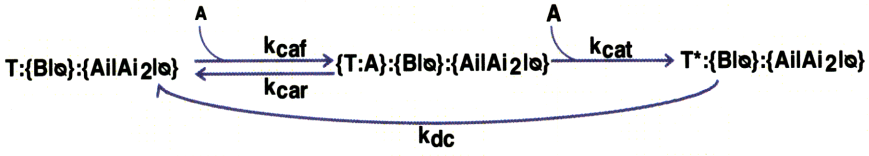
A
kcaf
T:{Blo}:{AilAi2lo}
{T:A}:{Blo}:{AilAi2lo}
A
kcat
T*:{Blo}:{AilAi2lo}
kcar
kdc

d

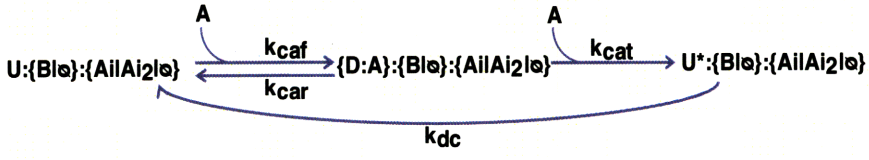
A
kcaf
U:{Blo}:{AilAi2lo}
{D:A}:{Blo}:{AilAi2lo}
A
kcat
U*:{Blo}:{AilAi2lo}
kcar
kdc

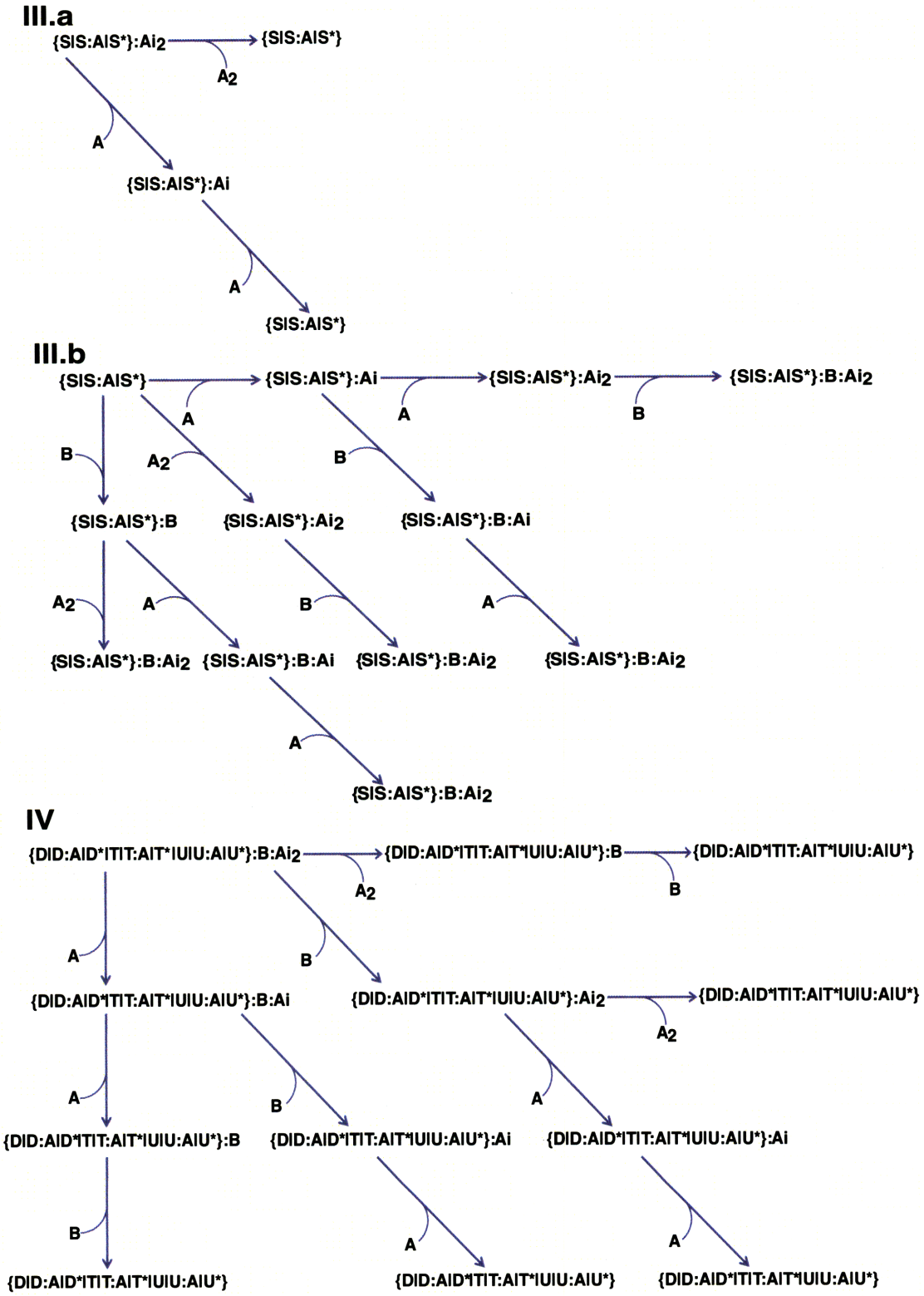
III.a
{SIS:AIS*}:Ai2
{SIS:AIS*}
A2
A
{SIS:AIS*}:Ai
A
{SIS:AIS*}
III.b
{SIS:AIS*}
{SIS:AIS*}:Ai
{SIS:AIS*}:Ai2
{SIS:AIS*}:B:Ai2
A
A
B
B
A2
B
{SIS:AIS*}:B
{SIS:AIS*}:Ai2
{SIS:AIS*}:B:Ai
A2
A
B
A
{SIS:AIS*}:B:Ai2
{SIS:AIS*}:B:Ai
{SIS:AIS*}:B:Ai2
{SIS:AIS*}:B:Ai2
A
{SIS:AIS*}:B:Ai2
IV
{DID:AID*ITIT:AIT*IUIU:AIU*}:B:Ai2
{DID:AID*ITIT:AIT*IUIU:AIU*}:B
{DID:AID*ITIT:AIT*IUIU:AIU*}
A2
B
A
B
{DID:AID*ITIT:AIT*IUIU:AIU*}:B:Ai
{DID:AID*ITIT:AIT*IUIU:AIU*}:Ai2
{DID:AID*ITIT:AIT*IUIU:AIU*}
A2
A
B
A
{DID:AID*ITIT:AIT*IUIU:AIU*}:B
{DID:AID*ITIT:AIT*IUIU:AIU*}:Ai
{DID:AID*ITIT:AIT*IUIU:AIU*}:Ai
B
A
A
{DID:AID*ITIT:AIT*IUIU:AIU*}
{DID:AID*ITIT:AIT*IUIU:AIU*}
{DID:AID*ITIT:AIT*IUIU:AIU*}

Figure A-1: **Full Graphical Description of the Mass Action Model.** (I) The model accounts for time-varying biochemical concentrations (state variables) of heteromultimeric complexes formed by the Kai proteins, along with the intermediate protein complexes, such as Michaelis complexes, within the autokinase and autophosphatase reactions of KaiC that maintain oscillation. (II) The reactions described here show the affect of KaiA allosteric regulation on KaiC activation, where the KaiA-bound KaiC form is the transition state from unactivated to activated KaiC. (III and IV) KaiABC complex assembly (III.b) and disassembly (III.a and IV) are accounted for by combinatorial intermediate binding states. The general principles are that (1) KaiB and KaiA can only assemble with the S-KaiC phosphoform, (2) KaiB can only disassemble from the D-KaiC, T-KaiC, and U-KaiC phosphoforms, and (3) KaiA may disassemble from any of the phosphoforms. A MATLAB implementation of the mathematical model is provided in the following appendix.

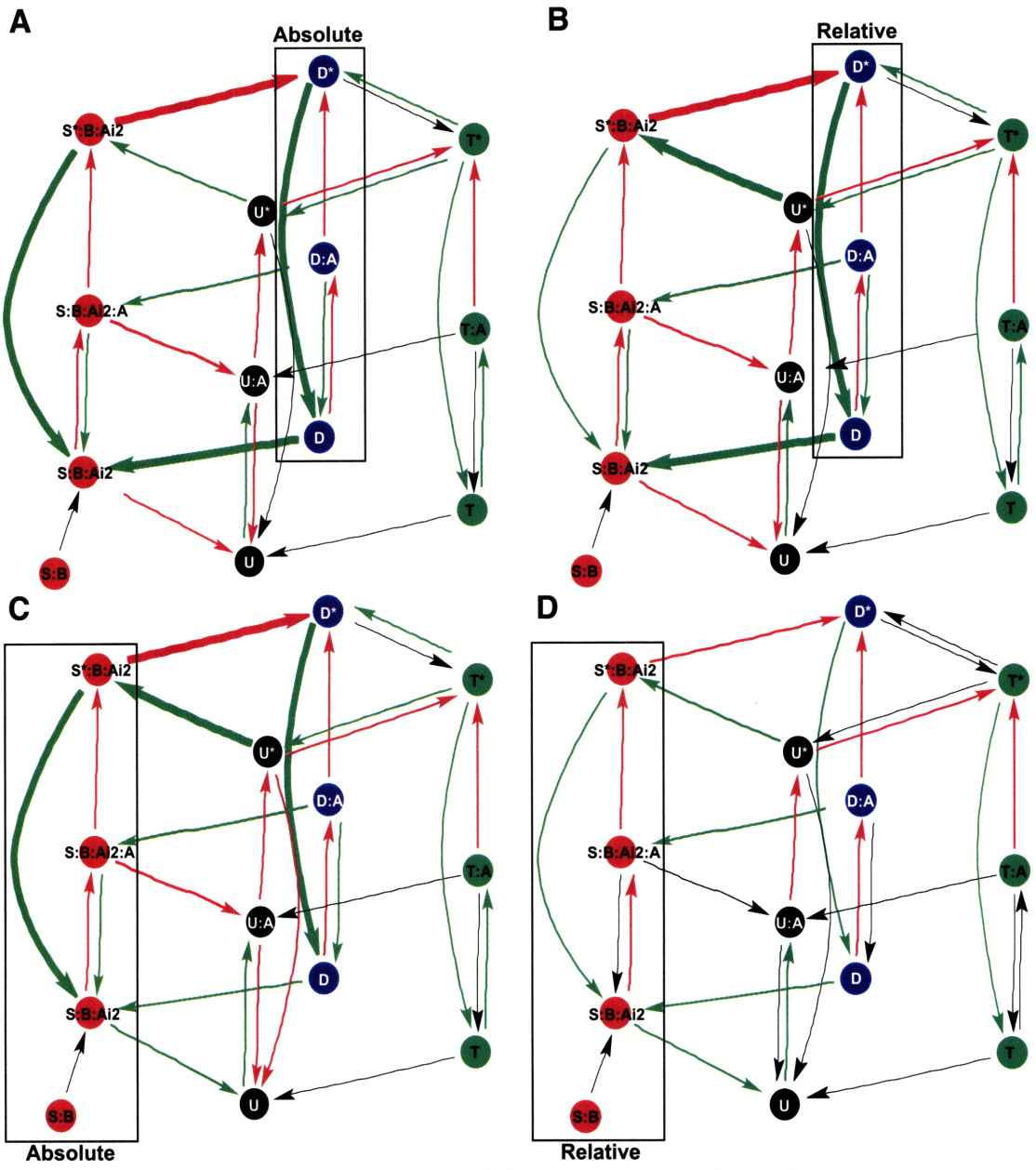
A
Absolute
B
Relative
C
Absolute
D
Relative
D*
S*:B:Ai2
T*
U*
D:A
S:B:Ai2:A
T:A
U:A
D
S:B:Ai2
T
U
S:B

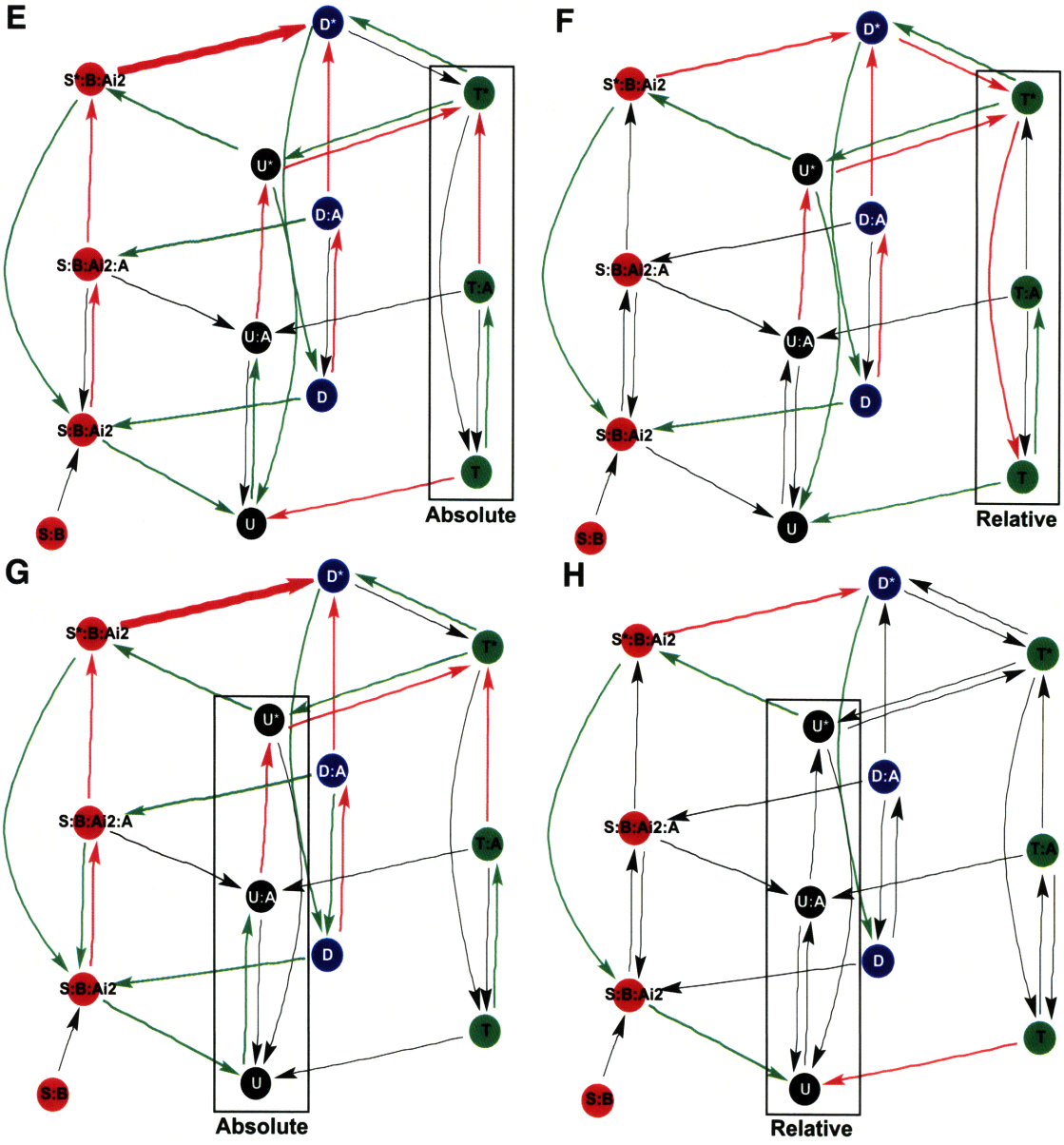

Figure A-2: **Scaled Absolute (left) and Scaled Relative (right) Amplitude Sensitivities** $\frac{\partial \log \alpha}{\partial \log p}$**.** The amplitude sensitivities are weighted logarithmically according to the same spread for period sensitivities in Figure 5-4. The absolute amplitude of a species is the concentration level and the relative amplitude is the difference between its maximum and minimum concentrations, where the concentration is periodic in time.

KaiABC Assembly and Disassembly Reactions	
No.	Biochemical Process
1	$B+\{S\|S:A\|S^*\}:\{Ai_n\|\emptyset\} \xrightarrow{k_{cbf}} \{S\|S:A\|S^*\}:B:\{Ai_n\|\emptyset\}$, $n \in \{1,2\}$
2	$A_2+\{S\|S:A\|S^*\}:B \xrightarrow{k_{sai}} \{S\|S:A\|S^*\}:B:Ai_2$
3	$A+\{S\|S:A\|S^*\}:B:Ai \xrightarrow{k_{sai2}} \{S\|S:A\|S^*\}:B:Ai_2$
4	$A_2 \xrightarrow{k_{db}} A+A$
5	$\{C\|C:A\|C^*\}:B:\{Ai_n\|\emptyset\} \xrightarrow{k_{cbr}} \{C\|C:A\|C^*\}:\{Ai_n\|\emptyset\}+B$, $C \in \{D,T,U\}$, $n \in \{1,2\}$
6	$\{C\|C:A\|C^*\}:\{B\|\emptyset\}:Ai_n \xrightarrow{k_{di}} \{C\|C:A\|C^*\}:\{B\|\emptyset\}+A_n$, $C \in \{D,T,U\}$, $n \in \{1,2\}$
	$\{S\|S:A\|S^*\}:Ai_n \xrightarrow{k_{di}} \{S\|S:A\|S^*\}+A_n$, $n \in \{1,2\}$

Table A.1: The assembly and disassembly reactions are shown here. The corresponding reaction rates are in Table A.5 and a graphical representation of the corresponding pathways is shown in Figures A-1(III) and A-1(IV).

KaiA Allosteric Regulation Reactions	
No.	Biochemical Process
7	C:{B|∅}:{Ai$_n$|∅}+A $\xrightarrow{k_{caf}}$ C:A:{B|∅}:{Ai$_n$|∅}, C ∈ {D,S,T,U}, n ∈ {1,2}
8	C:A:{B|∅}:{Ai$_n$|∅} $\xrightarrow{k_{car}}$ C:{B|∅}:{Ai$_n$|∅}+A, C ∈ {D,S,T,U}, n ∈ {1,2}
9	C:A:{B|∅}:{Ai$_n$|∅} $\xrightarrow{k_{cat}}$ C*:{B|∅}:{Ai$_n$|∅}+A, C ∈ {D,S,T,U}, n ∈ {1,2}
10	C*:{B|∅}:{Ai$_n$|∅} $\xrightarrow{k_{dc}}$ C:{B|∅}:{Ai$_n$|∅}, C ∈ {D,S,T,U}, n ∈ {1,2}

Table A.2: The KaiA allosteric regulation reactions are shown here. The corresponding reaction rates are in Table A.6 and a graphical representation of the corresponding pathways is shown in Figures A-1(II).

No.	Phosphoform Conversions with Basal Rates Biochemical Process
11	$\{U\|U{:}A\}{:}\{B\|\emptyset\}{:}\{Ai_n\|\emptyset\} \xrightarrow{k^0_{us}} \{S\|S{:}A\}{:}\{B\|\emptyset\}{:}\{Ai_n\|\emptyset\}$, $n \in \{1,2\}$
12	$\{U\|U{:}A\}{:}\{B\|\emptyset\}{:}\{Ai_n\|\emptyset\} \xrightarrow{k^0_{ut}} \{T\|T{:}A\}{:}\{B\|\emptyset\}{:}\{Ai_n\|\emptyset\}$, $n \in \{1,2\}$
13	$\{S\|S{:}A\}{:}\{B\|\emptyset\}{:}\{Ai_n\|\emptyset\} \xrightarrow{k^0_{sd}} \{D\|D{:}A\}{:}\{B\|\emptyset\}{:}\{Ai_n\|\emptyset\}$, $n \in \{1,2\}$
14	$\{T\|T{:}A\}{:}\{B\|\emptyset\}{:}\{Ai_n\|\emptyset\} \xrightarrow{k^0_{td}} \{D\|D{:}A\}{:}\{B\|\emptyset\}{:}\{Ai_n\|\emptyset\}$, $n \in \{1,2\}$
15	$\{S\|S{:}A\}{:}\{B\|\emptyset\}{:}\{Ai_n\|\emptyset\} \xrightarrow{k^0_{su}} \{U\|U{:}A\}{:}\{B\|\emptyset\}{:}\{Ai_n\|\emptyset\}$, $n \in \{1,2\}$
16	$\{T\|T{:}A\}{:}\{B\|\emptyset\}{:}\{Ai_n\|\emptyset\} \xrightarrow{k^0_{tu}} \{U\|U{:}A\}{:}\{B\|\emptyset\}{:}\{Ai_n\|\emptyset\}$, $n \in \{1,2\}$
17	$\{D\|D{:}A\}{:}\{B\|\emptyset\}{:}\{Ai_n\|\emptyset\} \xrightarrow{k^0_{ds}} \{S\|S{:}A\}{:}\{B\|\emptyset\}{:}\{Ai_n\|\emptyset\}$, $n \in \{1,2\}$
18	$\{D\|D{:}A\}{:}\{B\|\emptyset\}{:}\{Ai_n\|\emptyset\} \xrightarrow{k^0_{dt}} \{T\|T{:}A\}{:}\{B\|\emptyset\}{:}\{Ai_n\|\emptyset\}$, $n \in \{1,2\}$

Table A.3: The KaiC phosphoform interconversions at basal rates are shown here. The corresponding reaction rates are in Table A.7 and a graphical representation of the corresponding pathways is shown in Figure A-1(I).

Phosphoform Conversions with Maximal Effect of Free KaiA	
No.	Biochemical Process
19	$U^*:\{B\|\emptyset\}:\{Ai_n\|\emptyset\} \xrightarrow{k^1_{us}} S^*:\{B\|\emptyset\}:\{Ai_n\|\emptyset\}$, $n \in \{1,2\}$
20	$U^*:\{B\|\emptyset\}:\{Ai_n\|\emptyset\} \xrightarrow{k^1_{ut}} T^*:\{B\|\emptyset\}:\{Ai_n\|\emptyset\}$, $n \in \{1,2\}$
21	$S^*:\{B\|\emptyset\}:\{Ai_n\|\emptyset\} \xrightarrow{k^1_{sd}} D^*:\{B\|\emptyset\}:\{Ai_n\|\emptyset\}$, $n \in \{1,2\}$
22	$T^*:\{B\|\emptyset\}:\{Ai_n\|\emptyset\} \xrightarrow{k^1_{td}} D^*:\{B\|\emptyset\}:\{Ai_n\|\emptyset\}$, $n \in \{1,2\}$
23	$S^*:\{B\|\emptyset\}:\{Ai_n\|\emptyset\} \xrightarrow{k^1_{su}} U^*:\{B\|\emptyset\}:\{Ai_n\|\emptyset\}$, $n \in \{1,2\}$
24	$T^*:\{B\|\emptyset\}:\{Ai_n\|\emptyset\} \xrightarrow{k^1_{tu}} U^*:\{B\|\emptyset\}:\{Ai_n\|\emptyset\}$, $n \in \{1,2\}$
25	$D^*:\{B\|\emptyset\}:\{Ai_n\|\emptyset\} \xrightarrow{k^1_{ds}} S^*:\{B\|\emptyset\}:\{Ai_n\|\emptyset\}$, $n \in \{1,2\}$
26	$D^*:\{B\|\emptyset\}:\{Ai_n\|\emptyset\} \xrightarrow{k^1_{dt}} T^*:\{B\|\emptyset\}:\{Ai_n\|\emptyset\}$, $n \in \{1,2\}$

Table A.4: The KaiC phosphoform interconversions with maximal effect of free KaiA are shown here. The corresponding reaction rates are in Table A.8 and a graphical representation of the corresponding pathways is shown in Figure A-1(I).

KaiABC Assembly and Disassembly Reaction Rates			
Process No.	Param	Biochemical Role	Value
1	k_{cbf}	KaiB association to KaiABC complex	99999.999622 h^{-1}
2	k_{sai}	KaiA dimer inactivation and association to KaiABC complex	9999.429177 h^{-1}
3	k_{sai2}	KaiA monomer inactivation and association to KaiABC complex	1000000 h^{-1}
4	k_{db}	KaiA dimer dissociation into monomers	1651.394384 h^{-1}
5	k_{cbr}	KaiB dissociation rate from KaiABC complex	1000 h^{-1}
6	k_{di}	Inactive KaiA monomer and dimer dissociation from KaiABC complex (reactivation)	1005.404552 h^{-1}

Table A.5: The KaiABC assembly and disassembly occur at a much more rapid time scale in comparison to the KaiC phophoform interconversions.

KaiA Allosteric Regulation Reaction Rates			
Process No.	Param	Biochemical Role	Value
7	k_{caf}	Active KaiA monomer association to unmodified KaiC	6902.765488 h^{-1}
8	k_{car}	Active KaiA monomer dissociation from KaiA-bound KaiC	768.113739 h^{-1}
9	k_{cat}	KaiA-bound KaiC to KaiA dissociation and modified KaiC	2073.852642 h^{-1}
10	k_{dc}	Modified KaiC dissipation into unmodified KaiC	385.056804 h^{-1}

Table A.6: The KaiA allosteric regulation occurs at a much more rapid time scale in comparison to the KaiC phophoform interconversions and is at most an order of magnitude slower than KaiABC complexing.

Phosphoform Conversion Rates with Basal Effect			
Process No.	Param	Biochemical Role	Value
11	k^0_{us}	Unphosphorylated KaiC to Serine (S431) Phosphorylated KaiC	$0\,h^{-1}$
12	k^0_{ut}	Unphosphorylated KaiC to Threonine (T432) Phosphorylated KaiC	$0\,h^{-1}$
13	k^0_{sd}	Serine Phosphorylated KaiC to Serine and Threonine (Doubly) Phosphorylated KaiC	$0\,h^{-1}$
14	k^0_{td}	Threonine Phosphorylated KaiC to Serine and Threonine (Doubly) Phosphorylated KaiC	$0\,h^{-1}$
15	k^0_{su}	Serine Phosphorylated KaiC to Unphosphorylated KaiC	$0.111013\,h^{-1}$
16	k^0_{tu}	Threonine Phosphorylated KaiC to Unphosphorylated KaiC	$0.209541\,h^{-1}$
17	k^0_{ds}	Doubly Phosphorylated KaiC to Serine Phosphorylated KaiC	$0.307945\,h^{-1}$
18	k^0_{dt}	Doubly Phosphorylated KaiC to Threonine Phosphorylated KaiC	$0\,h^{-1}$

Table A.7: The KaiC phosphoform interconversions at the basal rate autodephosphorylate due to the absence of free KaiA. Due to the role that free KaiA plays in allosterically regulating KaiC phosphoform interconversions, no phosphorylation occurs without it.

Phosphoform Conversion Rates with Maximal Effect of free KaiA			
Process No.	Param	Biochemical Role	Value
19	k^1_{us}	Unphosphorylated KaiC to Serine (S431) Phosphorylated KaiC	$0.057680\,h^{-1}$
20	k^1_{ut}	Unphosphorylated KaiC to Threonine (T432) Phosphorylated KaiC	$0.477171\,h^{-1}$
21	k^1_{sd}	Serine Phosphorylated KaiC to Serine and Threonine (Doubly) Phosphorylated KaiC	$0.480154\,h^{-1}$
22	k^1_{td}	Threonine Phosphorylated KaiC to Serine and Threonine (Doubly) Phosphorylated KaiC	$0.201779\,h^{-1}$
23	k^1_{su}	Serine Phosphorylated KaiC to Unphosphorylated KaiC	$0\,h^{-1}$
24	k^1_{tu}	Threonine Phosphorylated KaiC to Unphosphorylated KaiC	$0.306751\,h^{-1}$
25	k^1_{ds}	Doubly Phosphorylated KaiC to Serine Phosphorylated KaiC	$0\,h^{-1}$
26	k^1_{dt}	Doubly Phosphorylated KaiC to Threonine Phosphorylated KaiC	$0.166900\,h^{-1}$

Table A.8: The KaiC phosphoform interconversions with maximal effect of free KaiA. Serine dephosphorylation does not occur due to the role that S-KaiC plays in sequestering free KaiA from the system.

Initial Concentrations		
Species	Value	Experiment
D_0	$1.36\,\mu M$	Figure 5-1A
S_0	$0.34\,\mu M$	
T_0	$0.68\,\mu M$	
U_0	$1.02\,\mu M$	
A_0	$1.3\,\mu M$	
B_0	$3.4\,\mu M$	
D_0	$0\,\mu M$	Figure 5-1B
S_0	$0\,\mu M$	
T_0	$0\,\mu M$	
U_0	$3.4\,\mu M$	
A_0	$1.3\,\mu M$	
B_0	$0\,\mu M$	
D_0	$0\,\mu M$	Figure 5-1C
S_0	$0.9\,\mu M$	
T_0	$0\,\mu M$	
U_0	$2.5\,\mu M$	
A_0	$1.3\,\mu M$	
B_0	$0\,\mu M$	
D_0	$1\,\mu M$	Figure 5-1D
S_0	$0.5\,\mu M$	
T_0	$0.7\,\mu M$	
U_0	$1.2\,\mu M$	
A_0	$0\,\mu M$	
B_0	$0\,\mu M$	

Table A.9: The initial concentrations of six of the state variables are provided here. The remainder of the 75 total state variables are initialized to zero.

Mass Conservation Matrix m			
Species	Protein		
	KaiA	KaiB	KaiC
B	0	1	0
A	1	0	0
Ai_2	2	0	0
D	0	0	1
S	0	0	1
T	0	0	1
U	0	0	1
D:A	1	0	1
S:A	1	0	1
T:A	1	0	1
U:A	1	0	1
D*	0	0	1
S*	0	0	1
T*	0	0	1
U*	0	0	1
D:Ai	1	0	1
S:Ai	1	0	1
T:Ai	1	0	1
U:Ai	1	0	1
D:Ai:A	2	0	1
S:Ai:A	2	0	1
T:Ai:A	2	0	1
U:Ai:A	2	0	1
D*:Ai	1	0	1
S*:Ai	1	0	1
T*:Ai	1	0	1
U*:Ai	1	0	1
$D:Ai_2$	2	0	1
$S:Ai_2$	2	0	1
$T:Ai_2$	2	0	1

U:Ai_2	2	0	1
D:Ai_2:A	3	0	1
S:Ai_2:A	3	0	1
T:Ai_2:A	3	0	1
U:Ai_2:A	3	0	1
D*:Ai_2	2	0	1
S*:Ai_2	2	0	1
T*:Ai_2	2	0	1
U*:Ai_2	2	0	1
D:B	0	1	1
S:B	0	1	1
T:B	0	1	1
U:B	0	1	1
D:B:A	1	1	1
S:B:A	1	1	1
T:B:A	1	1	1
U:B:A	1	1	1
D*:B	0	1	1
S*:B	0	1	1
T*:B	0	1	1
U*:B	0	1	1
D:B:Ai	1	1	1
S:B:Ai	1	1	1
T:B:Ai	1	1	1
U:B:Ai	1	1	1
D:B:Ai:A	2	1	1
S:B:Ai:A	2	1	1
T:B:Ai:A	2	1	1
U:B:Ai:A	2	1	1
D*:B:Ai	1	1	1
S*:B:Ai	1	1	1
T*:B:Ai	1	1	1
U*:B:Ai	1	1	1

D:B:Ai_2	2	1	1
S:B:Ai_2	2	1	1
T:B:Ai_2	2	1	1
U:B:Ai_2	2	1	1
D:B:Ai_2:A	3	1	1
S:B:Ai_2:A	3	1	1
T:B:Ai_2:A	3	1	1
U:B:Ai_2:A	3	1	1
D*:B:Ai_2	2	1	1
S*:B:Ai_2	2	1	1
T*:B:Ai_2	2	1	1
U*:B:Ai_2	2	1	1
$m^T \cdot y(t, p; y_0(p))$	$1.3\,\mu M$	$3.4\,\mu M$	$3.4\,\mu M$

Table A.10: The 75 state variables are listed here along with the mass conservation relationships to the total amounts of KaiA, KaiB, and KaiC for this post-translational oscillator.

KaiC Output Control Matrix c				
Species	KaiC Phosphoform			
	D-KaiC	S-KaiC	T-KaiC	U-KaiC
B	0	0	0	0
A	0	0	0	0
Ai_2	0	0	0	0
D	1	0	0	0
S	0	1	0	0
T	0	0	1	0
U	0	0	0	1
D:A	1	0	0	0
S:A	0	1	0	0
T:A	0	0	1	0
U:A	0	0	0	1
D*	1	0	0	0
S*	0	1	0	0
T*	0	0	1	0
U*	0	0	0	1
D:Ai	1	0	0	0
S:Ai	0	1	0	0
T:Ai	0	0	1	0
U:Ai	0	0	0	1
D:Ai:A	1	0	0	0
S:Ai:A	0	1	0	0
T:Ai:A	0	0	1	0
U:Ai:A	0	0	0	1
D*:Ai	1	0	0	0
S*:Ai	0	1	0	0
T*:Ai	0	0	1	0
U*:Ai	0	0	0	1
$D:Ai_2$	1	0	0	0
$S:Ai_2$	0	1	0	0
$T:Ai_2$	0	0	1	0

U:Ai_2	0	0	0	1
D:Ai_2:A	1	0	0	0
S:Ai_2:A	0	1	0	0
T:Ai_2:A	0	0	1	0
U:Ai_2:A	0	0	0	1
D*:Ai_2	1	0	0	0
S*:Ai_2	0	1	0	0
T*:Ai_2	0	0	1	0
U*:Ai_2	0	0	0	1
D:B	1	0	0	0
S:B	0	1	0	0
T:B	0	0	1	0
U:B	0	0	0	1
D:B:A	1	0	0	0
S:B:A	0	1	0	0
T:B:A	0	0	1	0
U:B:A	0	0	0	1
D*:B	1	0	0	0
S*:B	0	1	0	0
T*:B	0	0	1	0
U*:B	0	0	0	1
D:B:Ai	1	0	0	0
S:B:Ai	0	1	0	0
T:B:Ai	0	0	1	0
U:B:Ai	0	0	0	1
D:B:Ai:A	1	0	0	0
S:B:Ai:A	0	1	0	0
T:B:Ai:A	0	0	1	0
U:B:Ai:A	0	0	0	1
D*:B:Ai	1	0	0	0
S*:B:Ai	0	1	0	0
T*:B:Ai	0	0	1	0
U*:B:Ai	0	0	0	1

D:B:Ai_2	1	0	0	0
S:B:Ai_2	0	1	0	0
T:B:Ai_2	0	0	1	0
U:B:Ai_2	0	0	0	1
D:B:Ai_2:A	1	0	0	0
S:B:Ai_2:A	0	1	0	0
T:B:Ai_2:A	0	0	1	0
U:B:Ai_2:A	0	0	0	1
D*:B:Ai_2	1	0	0	0
S*:B:Ai_2	0	1	0	0
T*:B:Ai_2	0	0	1	0
U*:B:Ai_2	0	0	0	1

Table A.11: This control matrix captures the outputs of interest which are the four KaiC phosphoforms: serine and threonine phosphorylated KaiC (D-KaiC), serine phosphorylated KaiC (S-KaiC), threonine phosphorylated KaiC (T-KaiC), and unphosphorylated KaiC (U-KaiC). Alternative control matrices could be implemented to capture KaiABC complexing levels and any other outputs of interest.

Period Decomposition Reactions	
Process No.	Process
1_{expt}	$A+XE \underset{k_{rxe}}{\overset{k_{fxe}}{\rightleftharpoons}} A{:}XE$
2_{expt}	$A+A{:}XE \underset{k_{rxe}}{\overset{k_{fxe}}{\rightleftharpoons}} A_2{:}XE$
3_{expt}	$A_2{:}XE \xrightarrow{k_{cxe}} XE^*+A_2X$
4_{expt}	$A_2X \xrightarrow{k_{cxe}} A+A$
5_{expt}	$XE^*+X \underset{k_{rx}}{\overset{k_{fx}}{\rightleftharpoons}} XE{:}X$
6_{expt}	$XE{:}X \xrightarrow{k_{cx}} XE^*+X^*$
7_{expt}	$XE^* \xrightarrow{k_{dx}} XE$
8_{expt}	$X^* \xrightarrow{k_{dx}} X$
9_{expt}	$\{C\|C{:}A\|C^*\}{:}\{B\|\emptyset\}{:}\{Ai_n\|\emptyset\}+X^* \underset{k_{offx}}{\overset{k_{onx}}{\rightleftharpoons}} \{C\|C{:}A\|C^*\}{:}\{B\|\emptyset\}{:}\{Ai_n\|\emptyset\}{:}X^*$, $C \in \{D,S,T,U\}$, $n \in \{1,2\}$

Table A.12: These reactions implement an enzyme-driven switch-like behavior. This rapid process corresponds to the computational experiment in Figure 5-5 and the results in Figures 5-6 and 5-7.

Period Partitioning Reaction Rates		
Process No.	Param	Value
1_{expt},2_{expt}	k_{fxe}	100000 h^{-1}
1_{expt},2_{expt}	k_{rxe}	500000 h^{-1}
3_{expt},4_{expt}	k_{cxe}	10000000 h^{-1}
5_{expt}	k_{fx}	1000000 h^{-1}
5_{expt}	k_{rx}	100000 h^{-1}
6_{expt}	k_{cx}	100000 h^{-1}
7_{expt},8_{expt}	k_{dx}	10000 h^{-1}
9_{expt}	k_{onx}	50000 h^{-1}
9_{expt}	k_{offx}	1000 h^{-1}

Table A.13: These are the reaction rates for the enzyme cascade specified in the above table, Table A.12.

$$
\begin{aligned}
h &= \frac{T}{N} \\
y(t+h,p;y_0(p)) &= y(t,p;y_0(p)) + \frac{h}{2}\cdot\left(f(y(t,p;y_0(p))) + f(y(t+h,p;y_0(p)))\right) \\
\frac{\partial}{\partial y(0)}\left(y(t+h,p;y_0(p)) = y(t,p;y_0(p)) + \frac{h}{2}\cdot\left(f(y(t,p;y_0(p))) + f(y(t+h,p;y_0(p)))\right)\right) & \\
\frac{\partial y(t+h,p;y_0(p))}{\partial y_0} &= \frac{\partial y(t,p;y_0(p))}{\partial y_0} \\
&\quad + \frac{h}{2}\cdot\Big[\frac{\partial f(y(t,p;y_0(p)))}{\partial y}\cdot\frac{\partial y(t,p;y_0(p))}{\partial y_0} \\
&\quad + \frac{\partial f(y(t+h,p;y_0(p)))}{\partial y}\cdot\frac{\partial y(t+h,p;y_0(p))}{\partial y_0}\Big] \\
\frac{\partial y(t+h,p;y_0(p))}{\partial y_0} &= \Big[I + \frac{h}{2}\cdot\frac{\partial f(y(t,p;y_0(p)))}{\partial y}\Big]\cdot\frac{\partial y(t,p;y_0(p))}{\partial y_0} \\
&\quad \cdot\Big[I - \frac{h}{2}\cdot\frac{\partial f(y(t+h,p;y_0(p)))}{\partial y}\Big]^{-1}
\end{aligned}
\tag{A.1}
$$

Trapezoidal rule to compute the state-transition matrix. The trapezoidal rule was implemented to calculate the Monodromy matrix, $\mathbf{M} = \frac{\partial y(T,p;y_0(p))}{\partial y_0}$ in Equation 4.8 by dividing the period $T(p)$ into N uniform subintervals, h. The partial derivatives of the state variables y of the ILCO were computed simply due to the stepwise integrations which are each differentiated with respect to the initial conditions y_0.

$$
\begin{aligned}
h &= \frac{T}{N} \\
y(t+h,p;y_0(p)) &= y(t,p;y_0(p)) + \frac{h}{2}\cdot\left(f(y(t,p;y_0(p))) + f(y(t+h,p;y_0(p)))\right) \\
\frac{\partial}{\partial p}\big(y(t+h,p;y_0(p)) &= y(t,p;y_0(p)) + \frac{h}{2}\cdot\left(f(y(t,p;y_0(p))) + f(y(t+h,p;y_0(p)))\right)\big) \\
\frac{\partial y(t+h,p;y_0(p))}{\partial p} &= \frac{\partial y(t,p;y_0(p))}{\partial p} \\
&\quad + \frac{h}{2}\cdot\Big[\frac{\partial f(y(t,p;y_0(p)))}{\partial y}\cdot\frac{\partial y(t,p;y_0(p))}{\partial p} \\
&\quad + \frac{\partial f(y(t+h,p;y_0(p)))}{\partial p}\cdot\frac{\partial y(t+h,p;y_0(p))}{\partial p}\Big] \\
\frac{\partial y(t+h,p;y_0(p))}{\partial p} &= \Big[I + \frac{h}{2}\cdot\frac{\partial f(y(t,p;y_0(p)))}{\partial p}\Big]\cdot\frac{\partial y(t,p;y_0(p))}{\partial p} \\
&\quad \cdot\Big[I - \frac{h}{2}\cdot\frac{\partial f(y(t+h,p;y_0(p)))}{\partial p}\Big]^{-1}
\end{aligned}
\tag{A.2}
$$

Trapezoidal rule to compute the parametric sensitivities. The trapezoidal rule was implemented to calculate the parametric sensitivities $S(T(p),p;0) = \frac{\partial y(T,p;y_0(p))}{\partial p}$ in Equation 4.11 by dividing the period $T(p)$ into N uniform subintervals, h. The partial derivatives of the state variables y of the ILCO were computed simply due to the stepwise integrations which are each differentiated with respect to the initial conditions y_0.

$$\left.\frac{\partial \beta_i}{\partial p}\right|_p = -\left(c_i^T \cdot \frac{\partial f}{\partial y} \cdot \dot{y}(\beta_i(p), p; y_0(p))\right)^{-1} \cdot c_i^T \cdot \frac{\partial f}{\partial y} \cdot S\left(\beta_i(p), p; \left.\frac{\partial y_0}{\partial p}\right|_p\right) + c_i^T \cdot \frac{\partial f}{\partial y} \cdot M \cdot \frac{\partial y_0}{\partial p} + c_i^T \cdot \frac{\partial f}{\partial p} \tag{A.3}$$

Peak-to-peak phase sensitivities. The peak-to-peak phase sensitivities was calculated by taking the time difference between extrema in different outputs. The phase sensitivity of the i-th output is the partial derivative of the time lapse β differentiated with respect to the parameterization. β is defined as the time lapse between the extrema for $c_i^T \cdot y$ and the extrema for an output of reference,$c_j^T \cdot y$, locked at $t = 0$. Instead of calculating output specific sensitivities, the sensitivity for the i-th state variable may be calculated by replacing $c_i^T \cdot y$ with y_i.

$$\left.\frac{\partial \log \beta_{ji}}{\partial \log p}\right|_p = \left(\left.\frac{\partial \beta_i}{\partial p}\right|_p - \left.\frac{\partial \beta_j}{\partial p}\right|_p\right) \cdot \left(\frac{p}{t_i - t_j}\right)^T \tag{A.4}$$

Scaled peak-to-peak phase sensitivities. The scaled sensitivities are peak-to-peak phase sensitivities normalized to both the parameterization and the time lapse between the two peaking events. Instead of calculating output specific sensitivities, the sensitivity for the i-th state variable may be calculated by replacing $c_i^T \cdot y$ with y_i.

$$\left.\frac{\partial \log \gamma_{ji}}{\partial \log p}\right|_p = \frac{\beta_{ji}(p)}{T} \cdot \left(\left.\frac{\partial \log \beta_{ji}}{\partial \log p}\right|_p - \left.\frac{\partial \log T}{\partial \log p}\right|_p \right) \cdot \left(\left.\frac{\partial \beta_i}{\partial p}\right|_p - \left.\frac{\partial \beta_j}{\partial p}\right|_p \right) \cdot \left(\frac{p}{t_i - t_j} \right)^T \quad \text{(A.5)}$$

Scaled angular peak-to-peak phase sensitivities. The scaled angular sensitivities were calculated to be the change of the phase angle as a result of an infinitesimal parameter change, instead of describing the change in time lapse between two peaking events. The change of period was accounted for and normalized out. Instead of calculating output specific sensitivities, the sensitivity for the i-th state variable may be calculated by replacing $c_i^T \cdot y$ with y_i.

$$\left.\frac{\partial \alpha_i}{\partial p}\right|_p = c_i^T \cdot S\left(t, p; \left.\frac{\partial y_0}{\partial p}\right|_p\right) + c_i^T \cdot M \cdot \frac{\partial y_0}{\partial p} \tag{A.6}$$

Amplitude sensitivities. The amplitude sensitivities are the parital derivatives of the outputs $c_i^T \cdot y$ with respect to the parameterization at any given time t. Instead of calculating output specific sensitivities, the sensitivity for the i-th state variable may be calculated by replacing $c_i^T \cdot y$ with y_i.

$$\left.\frac{\partial \log \alpha_{i,abs}}{\partial \log p}\right|_p = \left.\frac{\partial \alpha_{i,t_{max}}}{\partial p}\right|_p \cdot \left(\frac{p}{(c_i^T \cdot y)_{i,t_{max}}}\right)^T \tag{A.7}$$

Scaled relative amplitude sensitivities. The relative sensitivities were computed as the difference between the sensitivities at the maximum and minimum of a given output, $c_i^T \cdot y$ at any given time t. The scaled relative amplitude sensitivities are the relative sensitivities normalized to both the parameterization and the difference in output concentration between the maximum and minimum quantities. Instead of calculating output specific sensitivities, the sensitivity for the i-th state variable may be calculated by replacing $c_i^T \cdot y$ with y_i.

$$\left.\frac{\partial \log \alpha_{i,rel}}{\partial \log p}\right|_p = \left(\left.\frac{\partial \alpha_{i,t_{max}}}{\partial p}\right|_p - \left.\frac{\partial \alpha_{i,t_{min}}}{\partial p}\right|_p\right) \cdot \left(\frac{p}{(c_i^T \cdot y)_{i,t_{max}} - (c_i^T \cdot y)_{i,t_{min}}}\right)^T \quad \text{(A.8)}$$

Scaled absolute amplitude sensitivities. The absolute sensitivities were computed as the sensitivities at the maximum of a given output, $c_i^T \cdot y$ at any given time t. The scaled absolute amplitude sensitivities are the absolute sensitivities normalized to both the parameterization and the difference in output concentration between the maximum and minimum quantities. Instead of calculating output specific sensitivities, the sensitivity for the i-th state variable may be calculated by replacing $c_i^T \cdot y$ with y_i.

Appendix B

Mathematical Model

$$
\begin{aligned}
\frac{d[B]}{dt} &= k_{cbr}\cdot[U:A:B:Ai]-k_{cbf}\cdot[S:A:Ai_2]\cdot[B]+k_{cbr}\cdot[T:A:B:Ai_2]\\
&+k_{cbr}\cdot[U^*:B:Ai]-k_{cbf}\cdot[S:Ai_2]\cdot[B]+k_{cbr}\cdot[D:B:Ai_2]\\
&+k_{cbr}\cdot[U:B:Ai]+k_{cbr}\cdot[D:A:B:Ai_2]-k_{cbf}\cdot[S^*:Ai_2]\cdot[B]\\
&+k_{cbr}\cdot[D^*:B:Ai]+k_{cbr}\cdot[D:A:B:Ai]+k_{cbr}\cdot[D^*:B:Ai_2]\\
&-k_{cbf}\cdot[S]\cdot[B]+k_{cbr}\cdot[T:B:Ai_2]+k_{cbr}\cdot[U:B:Ai_2]\\
&+k_{cbr}\cdot[U^*:B:Ai_2]+k_{cbr}\cdot[T^*:B:Ai]+k_{cbr}\cdot[T:A:B:Ai]\\
&-k_{cbf}\cdot[S^*:Ai]\cdot[B]+k_{cbr}\cdot[D:A:B]+k_{cbr}\cdot[T:B]\\
&+k_{cbr}\cdot[U:B]+k_{cbr}\cdot[D:B]+k_{cbr}\cdot[T:A:B]\\
&+k_{cbr}\cdot[U:A:B]-k_{cbf}\cdot[S:A:Ai]\cdot[B]+k_{cbr}\cdot[T^*:B]\\
&+k_{cbr}\cdot[D^*:B]+k_{cbr}\cdot[T^*:B:Ai_2]+k_{cbr}\cdot[U:A:B:Ai_2]\\
&+k_{cbr}\cdot[U^*:B]-k_{cbf}\cdot[S:Ai]\cdot[B]-k_{cbf}\cdot[S^*]\cdot[B]\\
&+k_{cbr}\cdot[D:B:Ai]-k_{cbf}\cdot[S:A]\cdot[B]+k_{cbr}\cdot[T:B:Ai]\\
\frac{d[A]}{dt} &= k_{di}\cdot[U^*:B:Ai]-k_{caf}\cdot[S:B:Ai_2]\cdot[A]-k_{sai2}\cdot[S:A:B:Ai]\cdot[A]\\
&+k_{di}\cdot[T:A:B:Ai_2]+k_{cat}\cdot[T:A:B:Ai_2]+k_{cat}\cdot[S:A:B:Ai_2]\\
&+k_{cat}\cdot[U:A:B:Ai]+k_{car}\cdot[T:A:Ai_2]-k_{caf}\cdot[T:B:Ai_2]\cdot[A]\\
&+k_{di}\cdot[D:A:B:Ai_2]+k_{di}\cdot[D:A:Ai]+k_{cat}\cdot[T:A:B:Ai]\\
&+k_{di}\cdot[D:Ai_2]-k_{caf}\cdot[T:B]\cdot[A]+k_{di}\cdot[T:A:B:Ai]
\end{aligned}
$$

$$-k_{caf} \cdot [U : B] \cdot [A] + k_{car} \cdot [S : A] + k_{cat} \cdot [S : A]$$

$$+k_{di} \cdot [T : Ai_2] - k_{sai} \cdot [S : A : B] \cdot [A] + k_{car} \cdot [U : A : Ai]$$

$$+k_{car} \cdot [T : A : B] + k_{di} \cdot [S : A : Ai] + k_{cat} \cdot [D : A : B]$$

$$+k_{di} \cdot [D^* : B : Ai] + k_{cat} \cdot [U : A : Ai_2] + k_{car} \cdot [D : A : B : Ai_2]$$

$$-k_{caf} \cdot [U : Ai_2] \cdot [A] + k_{di} \cdot [U^* : B : Ai_2] + k_{cat} \cdot [U : A : B]$$

$$+k_{car} \cdot [S : A : Ai_2] + k_{cat} \cdot [U : A : Ai] + k_{di} \cdot [T^* : Ai]$$

$$+k_{cat} \cdot [S : A : B] - k_{caf} \cdot [T : B : Ai] \cdot [A] + k_{di} \cdot [D : B : Ai_2]$$

$$+k_{car} \cdot [T : A : B : Ai] + k_{di} \cdot [S^* : Ai_2] + k_{cat} \cdot [T : A : Ai]$$

$$+k_{di} \cdot [U : A : Ai] + k_{di} \cdot [U : Ai_2] + k_{di} \cdot [U : A : Ai_2]$$

$$-k_{caf} \cdot [D : B : Ai_2] \cdot [A] + k_{di} \cdot [T : Ai] - k_{caf} \cdot [T] \cdot [A]$$

$$+k_{di} \cdot [D : B : Ai] + k_{di} \cdot [D^* : B : Ai_2] + k_{cat} \cdot [S : A : Ai_2]$$

$$-k_{caf} \cdot [S] \cdot [A] + k_{car} \cdot [T : A] + k_{cat} \cdot [T : A] + k_{cat} \cdot [S : A : B : Ai]$$

$$-k_{caf} \cdot [S : B : Ai] \cdot [A] + k_{di} \cdot [U : Ai] + k_{car} \cdot [U : A : B : Ai]$$

$$+k_{car} \cdot [S : A : B : Ai_2] - k_{caf} \cdot [D] \cdot [A] + k_{di} \cdot [D : A : B : Ai]$$

$$+k_{car} \cdot [D : A : B : Ai] + k_{car} \cdot [D : A : Ai_2] + k_{di} \cdot [T^* : B : Ai]$$

$$-k_{caf} \cdot [D : B] \cdot [A] + k_{car} \cdot [T : A : Ai] - k_{sai} \cdot [S^* : B] \cdot [A]$$

$$+k_{car} \cdot [U : A : Ai_2] + k_{di} \cdot [U^* : Ai] + k_{di} \cdot [D^* : Ai_2]$$

$$-k_{caf} \cdot [T : Ai] \cdot [A] + k_{di} \cdot [S : Ai_2] + k_{car} \cdot [T : A : B : Ai_2]$$

$$+k_{di} \cdot [D^* : Ai] + k_{car} \cdot [U : A] + k_{car} \cdot [D : A : B]$$

$$+k_{car} \cdot [S : A : B : Ai] - k_{sai2} \cdot [S : B : Ai] \cdot [A] - k_{caf} \cdot [T : Ai_2] \cdot [A]$$

$$-k_{caf} \cdot [D : Ai_2] \cdot [A] + k_{di} \cdot [T : A : Ai_2] + k_{cat} \cdot [D : A : Ai]$$

$$+k_{car} \cdot [U : A : B] + k_{cat} \cdot [U : A] + 2 \cdot k_{db} \cdot [A]i_2$$

$$+k_{car} \cdot [D : A] + k_{cat} \cdot [D : A] - k_{caf} \cdot [S : Ai] \cdot [A]$$

$$+k_{di} \cdot [S : A : Ai_2] + k_{cat} \cdot [D : A : B : Ai] + k_{di} \cdot [T : B : Ai_2]$$

$$+k_{di} \cdot [U : A : B : Ai] - k_{caf} \cdot [U : Ai] \cdot [A] + k_{di} \cdot [D : Ai]$$

$$
\begin{aligned}
& +k_{cat}\cdot[D:A:Ai_2]+k_{di}\cdot[D:A:Ai_2]+k_{cat}\cdot[S:A:Ai] \\
& +k_{di}\cdot[T:A:Ai]-k_{sai}\cdot[S:B]\cdot[A]-k_{caf}\cdot[U]\cdot[A] \\
& -k_{caf}\cdot[U:B:Ai]\cdot[A]+k_{car}\cdot[S:A:Ai]-k_{caf}\cdot[U:B:Ai_2]\cdot[A] \\
& +k_{car}\cdot[U:A:B:Ai_2]+k_{di}\cdot[S:Ai]+k_{di}\cdot[S^*:Ai] \\
& -k_{caf}\cdot[D:B:Ai]\cdot[A]-k_{caf}\cdot[D:Ai]\cdot[A]+k_{car}\cdot[S:A:B] \\
& +k_{di}\cdot[U:A:B:Ai_2]-k_{caf}\cdot[S:Ai_2]\cdot[A]+k_{cat}\cdot[U:A:B:Ai_2] \\
& +k_{car}\cdot[D:A:Ai]+k_{cat}\cdot[T:A:Ai_2]+k_{di}\cdot[U:B:Ai] \\
& +k_{di}\cdot[T^*:B:Ai_2]+k_{di}\cdot[U^*:Ai_2]-k_{caf}\cdot[S:B]\cdot[A] \\
& +k_{cat}\cdot[T:A:B]-k_{sai2}\cdot[S^*:B:Ai]\cdot[A]+k_{di}\cdot[T:B:Ai] \\
& +k_{di}\cdot[U:B:Ai_2]+k_{di}\cdot[T^*:Ai_2]+k_{cat}\cdot[D:A:B:Ai_2] \\
\frac{d[Ai_2]}{dt} &= k_{di}\cdot[T:A:B:Ai_2]-k_{sai}\cdot[S:A:B]\cdot[Ai_2]-k_{sai}\cdot[S:B]\cdot[Ai_2] \\
& +k_{di}\cdot[D:A:B:Ai_2]+k_{di}\cdot[D:Ai_2]+k_{di}\cdot[T:Ai_2] \\
& +k_{di}\cdot[U^*:B:Ai_2]+k_{di}\cdot[D:B:Ai_2]+k_{di}\cdot[S^*:Ai_2] \\
& +k_{di}\cdot[U:Ai_2]+k_{di}\cdot[U:A:Ai_2]+k_{di}\cdot[D^*:B:Ai_2] \\
& +k_{di}\cdot[D^*:Ai_2]+k_{di}\cdot[S:Ai_2]+k_{di}\cdot[T:A:Ai_2] \\
& -k_{db}\cdot[Ai_2]+k_{di}\cdot[S:A:Ai_2]+k_{di}\cdot[T:B:Ai_2] \\
& +k_{di}\cdot[D:A:Ai_2]+k_{di}\cdot[U:A:B:Ai_2]-k_{sai}\cdot[S^*:B]\cdot[Ai_2] \\
& +k_{di}\cdot[T^*:B:Ai_2]+k_{di}\cdot[U^*:Ai_2]+k_{di}\cdot[U:B:Ai_2] \\
& +k_{di}\cdot[T^*:Ai_2] \\
\frac{d[D]}{dt} &= -k^0_{ds}\cdot[D]-k^0_{dt}\cdot[D]+k^0_{sd}\cdot[S] \\
& +k^0_{td}\cdot[T]+k_{car}\cdot[D:A]+k_{dc}\cdot[D^*] \\
& +k_{di}\cdot[D:Ai]+k_{di}\cdot[D:Ai_2]+k_{cbr}\cdot[D:B] \\
& -k_{caf}\cdot[D]\cdot[A] \\
\frac{d[S]}{dt} &= k^0_{ds}\cdot[D]-k^0_{sd}\cdot[S]-k^0_{su}\cdot[S] \\
& +k^0_{us}\cdot[U]+k_{car}\cdot[S:A]+k_{dc}\cdot[S^*]
\end{aligned}
$$

$$
\begin{aligned}
& & & +k_{di} \cdot [S : Ai] + k_{di} \cdot [S : Ai_2] - k_{cbf} \cdot [S] \cdot [B] \\
& & & -k_{caf} \cdot [S] \cdot [A] \\
\frac{d[T]}{dt} & = & & k^0_{dt} \cdot [D] - k^0_{td} \cdot [T] - k^0_{tu} \cdot [T] \\
& & & +k^0_{ut} \cdot [U] + k_{car} \cdot [T : A] + k_{dc} \cdot [T^*] \\
& & & +k_{di} \cdot [T : Ai] + k_{di} \cdot [T : Ai_2] + k_{cbr} \cdot [T : B] \\
& & & -k_{caf} \cdot [T] \cdot [A] \\
\frac{d[U]}{dt} & = & & k^0_{su} \cdot [S] + k^0_{tu} \cdot [T] - k^0_{us} \cdot [U] \\
& & & -k^0_{ut} \cdot [U] + k_{car} \cdot [U : A] + k_{dc} \cdot [U^*] \\
& & & +k_{di} \cdot [U : Ai] + k_{di} \cdot [U : Ai_2] + k_{cbr} \cdot [U : B] \\
& & & -k_{caf} \cdot [U] \cdot [A] \\
\frac{d[D : A]}{dt} & = & & -k_{car} \cdot [D : A] - k^0_{ds} \cdot [D : A] - k^0_{dt} \cdot [D : A] \\
& & & -k_{cat} \cdot [D : A] + k^0_{sd} \cdot [S : A] + k^0_{td} \cdot [T : A] \\
& & & +k_{di} \cdot [D : A : Ai] + k_{di} \cdot [D : A : Ai_2] + k_{cbr} \cdot [D : A : B] \\
& & & +k_{caf} \cdot [D] \cdot [A] \\
\frac{d[S : A]}{dt} & = & & k^0_{ds} \cdot [D : A] - k_{car} \cdot [S : A] - k^0_{sd} \cdot [S : A] \\
& & & -k^0_{su} \cdot [S : A] - k_{cat} \cdot [S : A] + k^0_{us} \cdot [U : A] \\
& & & +k_{di} \cdot [S : A : Ai] + k_{di} \cdot [S : A : Ai_2] - k_{cbf} \cdot [S : A] \cdot [B] \\
& & & +k_{caf} \cdot [S] \cdot [A] \\
\frac{d[T : A]}{dt} & = & & k^0_{dt} \cdot [D : A] - k_{car} \cdot [T : A] - k^0_{td} \cdot [T : A] \\
& & & -k^0_{tu} \cdot [T : A] - k_{cat} \cdot [T : A] + k^0_{ut} \cdot [U : A] \\
& & & +k_{di} \cdot [T : A : Ai] + k_{di} \cdot [T : A : Ai_2] + k_{cbr} \cdot [T : A : B] \\
& & & +k_{caf} \cdot [T] \cdot [A] \\
\frac{d[U : A]}{dt} & = & & k^0_{su} \cdot [S : A] + k^0_{tu} \cdot [T : A] - k_{car} \cdot [U : A] \\
& & & -k^0_{us} \cdot [U : A] - k^0_{ut} \cdot [U : A] - k_{cat} \cdot [U : A] \\
& & & +k_{di} \cdot [U : A : Ai] + k_{di} \cdot [U : A : Ai_2] + k_{cbr} \cdot [U : A : B]
\end{aligned}
$$

$$
\begin{aligned}
& & & +k_{caf} \cdot [U] \cdot [A] \\
\frac{d[D^*]}{dt} &= & & k_{cat} \cdot [D : A] - k^1_{ds} \cdot [D^*] - k^1_{dt} \cdot [D^*] \\
& & & -k_{dc} \cdot [D^*] + k^1_{sd} \cdot [S^*] + k^1_{td} \cdot [T^*] \\
& & & +k_{di} \cdot [D^* : Ai] + k_{di} \cdot [D^* : Ai_2] + k_{cbr} \cdot [D^* : B] \\
\frac{d[S^*]}{dt} &= & & k_{cat} \cdot [S : A] + k^1_{ds} \cdot [D^*] - k^1_{sd} \cdot [S^*] \\
& & & -k^1_{su} \cdot [S^*] - k_{dc} \cdot [S^*] + k^1_{us} \cdot [U^*] \\
& & & +k_{di} \cdot [S^* : Ai] + k_{di} \cdot [S^* : Ai_2] - k_{cbf} \cdot [S^*] \cdot [B] \\
\frac{d[T^*]}{dt} &= & & k_{cat} \cdot [T : A] + k^1_{dt} \cdot [D^*] - k^1_{td} \cdot [T^*] \\
& & & -k^1_{tu} \cdot [T^*] - k_{dc} \cdot [T^*] + k^1_{ut} \cdot [U^*] \\
& & & +k_{di} \cdot [T^* : Ai] + k_{di} \cdot [T^* : Ai_2] + k_{cbr} \cdot [T^* : B] \\
\frac{d[U^*]}{dt} &= & & k_{cat} \cdot [U : A] + k^1_{su} \cdot [S^*] + k^1_{tu} \cdot [T^*] \\
& & & -k^1_{us} \cdot [U^*] - k^1_{ut} \cdot [U^*] - k_{dc} \cdot [U^*] \\
& & & +k_{di} \cdot [U^* : Ai] + k_{di} \cdot [U^* : Ai_2] + k_{cbr} \cdot [U^* : B] \\
\frac{d[D : Ai]}{dt} &= & & -k^0_{ds} \cdot [D : Ai] - k^0_{dt} \cdot [D : Ai] - k_{di} \cdot [D : Ai] \\
& & & +k^0_{sd} \cdot [S : Ai] + k^0_{td} \cdot [T : Ai] + k_{car} \cdot [D : A : Ai] \\
& & & +k_{dc} \cdot [D^* : Ai] + k_{di} \cdot [D : Ai_2] + k_{cbr} \cdot [D : B : Ai] \\
& & & -k_{caf} \cdot [D : Ai] \cdot [A] \\
\frac{d[S : Ai]}{dt} &= & & k^0_{ds} \cdot [D : Ai] - k^0_{sd} \cdot [S : Ai] - k^0_{su} \cdot [S : Ai] \\
& & & -k_{di} \cdot [S : Ai] + k^0_{us} \cdot [U : Ai] + k_{car} \cdot [S : A : Ai] \\
& & & +k_{dc} \cdot [S^* : Ai] + k_{di} \cdot [S : Ai_2] - k_{cbf} \cdot [S : Ai] \cdot [B] \\
& & & -k_{caf} \cdot [S : Ai] \cdot [A] \\
\frac{d[T : Ai]}{dt} &= & & k^0_{dt} \cdot [D : Ai] - k^0_{td} \cdot [T : Ai] - k^0_{tu} \cdot [T : Ai] \\
& & & -k_{di} \cdot [T : Ai] + k^0_{ut} \cdot [U : Ai] + k_{car} \cdot [T : A : Ai] \\
& & & +k_{dc} \cdot [T^* : Ai] + k_{di} \cdot [T : Ai_2] + k_{cbr} \cdot [T : B : Ai] \\
& & & -k_{caf} \cdot [T : Ai] \cdot [A]
\end{aligned}
$$

$$
\begin{aligned}
\frac{d[U:Ai]}{dt} &= k^0_{su}\cdot[S:Ai] + k^0_{tu}\cdot[T:Ai] - k^0_{us}\cdot[U:Ai] \\
&\quad -k^0_{ut}\cdot[U:Ai] - k_{di}\cdot[U:Ai] + k_{car}\cdot[U:A:Ai] \\
&\quad +k_{dc}\cdot[U^*:Ai] + k_{di}\cdot[U:Ai_2] + k_{cbr}\cdot[U:B:Ai] \\
&\quad -k_{caf}\cdot[U:Ai]\cdot[A] \\
\frac{d[D:A:Ai]}{dt} &= -k_{car}\cdot[D:A:Ai] - k^0_{ds}\cdot[D:A:Ai] - k^0_{dt}\cdot[D:A:Ai] \\
&\quad -k_{di}\cdot[D:A:Ai] - k_{cat}\cdot[D:A:Ai] + k^0_{sd}\cdot[S:A:Ai] \\
&\quad +k^0_{td}\cdot[T:A:Ai] + k_{di}\cdot[D:A:Ai_2] + k_{cbr}\cdot[D:A:B:Ai] \\
&\quad +k_{caf}\cdot[D:Ai]\cdot[A] \\
\frac{d[S:A:Ai]}{dt} &= k^0_{ds}\cdot[D:A:Ai] - k_{car}\cdot[S:A:Ai] - k^0_{sd}\cdot[S:A:Ai] \\
&\quad -k^0_{su}\cdot[S:A:Ai] - k_{di}\cdot[S:A:Ai] - k_{cat}\cdot[S:A:Ai] \\
&\quad +k^0_{us}\cdot[U:A:Ai] + k_{di}\cdot[S:A:Ai_2] - k_{cbf}\cdot[S:A:Ai]\cdot[B] \\
&\quad +k_{caf}\cdot[S:Ai]\cdot[A] \\
\frac{d[T:Ai:A]}{dt} &= k^0_{dt}\cdot[D:A:Ai] - k_{car}\cdot[T:A:Ai] - k^0_{td}\cdot[T:A:Ai] \\
&\quad -k^0_{tu}\cdot[T:A:Ai] - k_{di}\cdot[T:A:Ai] - k_{cat}\cdot[T:A:Ai] \\
&\quad +k^0_{ut}\cdot[U:A:Ai] + k_{di}\cdot[T:A:Ai_2] + k_{cbr}\cdot[T:A:B:Ai] \\
&\quad +k_{caf}\cdot[T:Ai]\cdot[A] \\
\frac{d[U:Ai:A]}{dt} &= k^0_{su}\cdot[S:A:Ai] + k^0_{tu}\cdot[T:A:Ai] - k_{car}\cdot[U:A:Ai] \\
&\quad -k^0_{us}\cdot[U:A:Ai] - k^0_{ut}\cdot[U:A:Ai] - k_{di}\cdot[U:A:Ai] \\
&\quad -k_{cat}\cdot[U:A:Ai] + k_{di}\cdot[U:A:Ai_2] + k_{cbr}\cdot[U:A:B:Ai] \\
&\quad +k_{caf}\cdot[U:Ai]\cdot[A] \\
\frac{d[D^*:Ai]}{dt} &= k_{cat}\cdot[D:A:Ai] - k^1_{ds}\cdot[D^*:Ai] - k^1_{dt}\cdot[D^*:Ai] \\
&\quad -k_{di}\cdot[D^*:Ai] - k_{dc}\cdot[D^*:Ai] + k^1_{sd}\cdot[S^*:Ai] \\
&\quad +k^1_{td}\cdot[T^*:Ai] + k_{di}\cdot[D^*:Ai_2] + k_{cbr}\cdot[D^*:B:Ai]
\end{aligned}
$$

$$
\begin{aligned}
\frac{d[S^* : Ai]}{dt} &= k_{cat} \cdot [S : A : Ai] + k^1_{ds} \cdot [D^* : Ai] - k^1_{sd} \cdot [S^* : Ai] \\
&\quad -k^1_{su} \cdot [S^* : Ai] - k_{di} \cdot [S^* : Ai] - k_{dc} \cdot [S^* : Ai] \\
&\quad +k^1_{us} \cdot [U^* : Ai] + k_{di} \cdot [S^* : Ai_2] - k_{cbf} \cdot [S^* : Ai] \cdot [B] \\
\frac{d[T^* : Ai]}{dt} &= k_{cat} \cdot [T : A : Ai] + k^1_{dt} \cdot [D^* : Ai] - k^1_{td} \cdot [T^* : Ai] \\
&\quad -k^1_{tu} \cdot [T^* : Ai] - k_{di} \cdot [T^* : Ai] - k_{dc} \cdot [T^* : Ai] \\
&\quad +k^1_{ut} \cdot [U^* : Ai] + k_{di} \cdot [T^* : Ai_2] + k_{cbr} \cdot [T^* : B : Ai] \\
\frac{d[U^* : Ai]}{dt} &= k_{cat} \cdot [U : A : Ai] + k^1_{su} \cdot [S^* : Ai] + k^1_{tu} \cdot [T^* : Ai] - k^1_{us} \cdot [U^* : Ai] \\
&\quad -k^1_{ut} \cdot [U^* : Ai] - k_{di} \cdot [U^* : Ai] - k_{dc} \cdot [U^* : Ai] \\
&\quad +k_{di} \cdot [U^* : Ai_2] + k_{cbr} \cdot [U^* : B : Ai] \\
\frac{d[D : Ai_2]}{dt} &= -k^0_{ds} \cdot [D : Ai_2] - k^0_{dt} \cdot [D : Ai_2] - 2 \cdot k_{di} \cdot [D : Ai_2] \\
&\quad +k^0_{sd} \cdot [S : Ai_2] + k^0_{td} \cdot [T : Ai_2] + k_{car} \cdot [D : A : Ai_2] \\
&\quad +k_{dc} \cdot [D^* : Ai_2] + k_{cbr} \cdot [D : B : Ai_2] - k_{caf} \cdot [D : Ai_2] \cdot [A] \\
\frac{d[S : Ai_2]}{dt} &= k^0_{ds} \cdot [D : Ai_2] - k^0_{sd} \cdot [S : Ai_2] - k^0_{su} \cdot [S : Ai_2] \\
&\quad -2 \cdot k_{di} \cdot [S : Ai_2] + k^0_{us} \cdot [U : Ai_2] + k_{car} \cdot [S : A : Ai_2] \\
&\quad +k_{dc} \cdot [S^* : Ai_2] - k_{cbf} \cdot [S : Ai_2] \cdot [B] - k_{caf} \cdot [S : Ai_2] \cdot [A] \\
\frac{d[T : Ai_2]}{dt} &= k^0_{dt} \cdot [D : Ai_2] - k^0_{td} \cdot [T : Ai_2] - k^0_{tu} \cdot [T : Ai_2] \\
&\quad -2 \cdot k_{di} \cdot [T : Ai_2] + k^0_{ut} \cdot [U : Ai_2] + k_{car} \cdot [T : A : Ai_2] \\
&\quad +k_{dc} \cdot [T^* : Ai_2] + k_{cbr} \cdot [T : B : Ai_2] - k_{caf} \cdot [T : Ai_2] \cdot [A] \\
\frac{d[U : Ai_2]}{dt} &= k^0_{su} \cdot [S : Ai_2] + k^0_{tu} \cdot [T : Ai_2] - k^0_{us} \cdot [U : Ai_2] \\
&\quad -k^0_{ut} \cdot [U : Ai_2] - 2 \cdot k_{di} \cdot [U : Ai_2] + k_{car} \cdot [U : A : Ai_2] \\
&\quad +k_{dc} \cdot [U^* : Ai_2] + k_{cbr} \cdot [U : B : Ai_2] - k_{caf} \cdot [U : Ai_2] \cdot [A] \\
\frac{d[D : A : Ai_2]}{dt} &= -k_{car} \cdot [D : A : Ai_2] - k^0_{ds} \cdot [D : A : Ai_2] - k^0_{dt} \cdot [D : A : Ai_2] \\
&\quad -2 \cdot k_{di} \cdot [D : A : Ai_2] - k_{cat} \cdot [D : A : Ai_2] + k^0_{sd} \cdot [S : A : Ai_2] \\
&\quad +k^0_{td} \cdot [T : A : Ai_2] + k_{cbr} \cdot [D : A : B : Ai_2] + k_{caf} \cdot [D : Ai_2] \cdot [A
\end{aligned}
$$

$$
\begin{aligned}
\frac{d[S:A:Ai_2]}{dt} &= k^0_{ds}\cdot[D:A:Ai_2] - k_{car}\cdot[S:A:Ai_2] - k^0_{sd}\cdot[S:A:Ai_2] \\
&\quad -k^0_{su}\cdot[S:A:Ai_2] - 2\cdot k_{di}\cdot[S:A:Ai_2] - k_{cat}\cdot[S:A:Ai_2] \\
&\quad +k^0_{us}\cdot[U:A:Ai_2] - k_{cbf}\cdot[S:A:Ai_2]\cdot[B] + k_{caf}\cdot[S:Ai_2]\cdot[A] \\
\frac{d[T:A:Ai_2]}{dt} &= k^0_{dt}\cdot[D:A:Ai_2] - k_{car}\cdot[T:A:Ai_2] - k^0_{td}\cdot[T:A:Ai_2] \\
&\quad -k^0_{tu}\cdot[T:A:Ai_2] - 2\cdot k_{di}\cdot[T:A:Ai_2] - k_{cat}\cdot[T:A:Ai_2] \\
&\quad +k^0_{ut}\cdot[U:A:Ai_2] + k_{cbr}\cdot[T:A:B:Ai_2] + k_{caf}\cdot[T:Ai_2]\cdot[A] \\
\frac{d[U:A:Ai_2]}{dt} &= k^0_{su}\cdot[S:A:Ai_2] + k^0_{tu}\cdot[T:A:Ai_2] - k_{car}\cdot[U:A:Ai_2] \\
&\quad -k^0_{us}\cdot[U:A:Ai_2] - k^0_{ut}\cdot[U:A:Ai_2] - 2\cdot k_{di}\cdot[U:A:Ai_2] \\
&\quad -k_{cat}\cdot[U:A:Ai_2] + k_{cbr}\cdot[U:A:B:Ai_2] + k_{caf}\cdot[U:Ai_2]\cdot[A] \\
\frac{d[D^*:Ai_2]}{dt} &= k_{cat}\cdot[D:A:Ai_2] - k^1_{ds}\cdot[D^*:Ai_2] - k^1_{dt}\cdot[D^*:Ai_2] \\
&\quad -2\cdot k_{di}\cdot[D^*:Ai_2] - k_{dc}\cdot[D^*:Ai_2] + k^1_{sd}\cdot[S^*:Ai_2] \\
&\quad +k^1_{td}\cdot[T^*:Ai_2] + k_{cbr}\cdot[D^*:B:Ai_2] \\
\frac{d[S^*:Ai_2]}{dt} &= k_{cat}\cdot[S:A:Ai_2] + k^1_{ds}\cdot[D^*:Ai_2] - k^1_{sd}\cdot[S^*:Ai_2] \\
&\quad -k^1_{su}\cdot[S^*:Ai_2] - 2\cdot k_{di}\cdot[S^*:Ai_2] - k_{dc}\cdot[S^*:Ai_2] \\
&\quad +k^1_{us}\cdot[U^*:Ai_2] - k_{cbf}\cdot[S^*:Ai_2]\cdot[B] \\
\frac{d[T^*:Ai_2]}{dt} &= k_{cat}\cdot[T:A:Ai_2] + k^1_{dt}\cdot[D^*:Ai_2] - k^1_{td}\cdot[T^*:Ai_2] \\
&\quad -k^1_{tu}\cdot[T^*:Ai_2] - 2\cdot k_{di}\cdot[T^*:Ai_2] - k_{dc}\cdot[T^*:Ai_2] \\
&\quad +k^1_{ut}\cdot[U^*:Ai_2] + k_{cbr}\cdot[T^*:B:Ai_2] \\
\frac{d[U^*:Ai_2]}{dt} &= k_{cat}\cdot[U:A:Ai_2] + k^1_{su}\cdot[S^*:Ai_2] + k^1_{tu}\cdot[T^*:Ai_2] \\
&\quad -k^1_{us}\cdot[U^*:Ai_2] - k^1_{ut}\cdot[U^*:Ai_2] - 2\cdot k_{di}\cdot[U^*:Ai_2] \\
&\quad -k_{dc}\cdot[U^*:Ai_2] + k_{cbr}\cdot[U^*:B:Ai_2] \\
\frac{d[D:B]}{dt} &= -k_{cbr}\cdot[D:B] - k^0_{ds}\cdot[D:B] - k^0_{dt}\cdot[D:B] + k^0_{sd}\cdot[S:B] \\
&\quad +k^0_{td}\cdot[T:B] + k_{car}\cdot[D:A:B] + k_{dc}\cdot[D^*:B] \\
&\quad +k_{di}\cdot[D:B:Ai] + k_{di}\cdot[D:B:Ai_2] - k_{caf}\cdot[D:B]\cdot[A]
\end{aligned}
$$

$$
\begin{aligned}
\frac{d[S:B]}{dt} &= k^0_{ds}\cdot[D:B] - k^0_{sd}\cdot[S:B] - k^0_{su}\cdot[S:B] + k^0_{us}\cdot[U:B] \\
&\quad + k_{car}\cdot[S:A:B] + k_{dc}\cdot[S^*:B] + k_{cbf}\cdot[S]\cdot[B] \\
&\quad - k_{caf}\cdot[S:B]\cdot[A] - k_{sai}\cdot[S:B]\cdot[A] - k_{sai}\cdot[S:B]\cdot[Ai_2] \\
\frac{d[T:B]}{dt} &= k^0_{dt}\cdot[D:B] - k_{cbr}\cdot[T:B] - k^0_{td}\cdot[T:B] \\
&\quad - k^0_{tu}\cdot[T:B] + k^0_{ut}\cdot[U:B] + k_{car}\cdot[T:A:B] \\
&\quad + k_{dc}\cdot[T^*:B] + k_{di}\cdot[T:B:Ai] + k_{di}\cdot[T:B:Ai_2] \\
&\quad - k_{caf}\cdot[T:B]\cdot[A] \\
\frac{d[U:B]}{dt} &= k^0_{su}\cdot[S:B] + k^0_{tu}\cdot[T:B] - k_{cbr}\cdot[U:B] \\
&\quad - k^0_{us}\cdot[U:B] - k^0_{ut}\cdot[U:B] + k_{car}\cdot[U:A:B] \\
&\quad + k_{dc}\cdot[U^*:B] + k_{di}\cdot[U:B:Ai] + k_{di}\cdot[U:B:Ai_2] \\
&\quad - k_{caf}\cdot[U:B]\cdot[A] \\
\frac{d[D:A:B]}{dt} &= -k_{cbr}\cdot[D:A:B] - k_{car}\cdot[D:A:B] - k^0_{ds}\cdot[D:A:B] \\
&\quad - k^0_{dt}\cdot[D:A:B] - k_{cat}\cdot[D:A:B] + k^0_{sd}\cdot[S:A:B] \\
&\quad + k^0_{td}\cdot[T:A:B] + k_{di}\cdot[D:A:B:Ai] + k_{di}\cdot[D:A:B:Ai_2] \\
&\quad + k_{caf}\cdot[D:B]\cdot[A] \\
\frac{d[S:A:B]}{dt} &= k^0_{ds}\cdot[D:A:B] - k_{car}\cdot[S:A:B] - k^0_{sd}\cdot[S:A:B] \\
&\quad - k^0_{su}\cdot[S:A:B] - k_{cat}\cdot[S:A:B] + k^0_{us}\cdot[U:A:B] \\
&\quad + k_{cbf}\cdot[S:A]\cdot[B] + k_{caf}\cdot[S:B]\cdot[A] - k_{sai}\cdot[S:A:B]\cdot[A] \\
&\quad - k_{sai}\cdot[S:A:B]\cdot[Ai_2] \\
\frac{d[T:A:B]}{dt} &= k^0_{dt}\cdot[D:A:B] - k_{cbr}\cdot[T:A:B] - k_{car}\cdot[T:A:B] \\
&\quad - k^0_{td}\cdot[T:A:B] - k^0_{tu}\cdot[T:A:B] - k_{cat}\cdot[T:A:B] \\
&\quad + k^0_{ut}\cdot[U:A:B] + k_{di}\cdot[T:A:B:Ai] + k_{di}\cdot[T:A:B:Ai_2] \\
&\quad + k_{caf}\cdot[T:B]\cdot[A]
\end{aligned}
$$

$$
\begin{aligned}
\frac{d[U:A:B]}{dt} &= k^0_{su}\cdot[S:A:B] + k^0_{tu}\cdot[T:A:B] - k_{cbr}\cdot[U:A:B] \\
&\quad -k_{car}\cdot[U:A:B] - k^0_{us}\cdot[U:A:B] - k^0_{ut}\cdot[U:A:B] \\
&\quad -k_{cat}\cdot[U:A:B] + k_{di}\cdot[U:A:B:Ai] + k_{di}\cdot[U:A:B:Ai_2] \\
&\quad +k_{caf}\cdot[U:B]\cdot[A] \\
\frac{d[D^*:B]}{dt} &= k_{cat}\cdot[D:A:B] - k_{cbr}\cdot[D^*:B] - k^1_{ds}\cdot[D^*:B] \\
&\quad -k^1_{dt}\cdot[D^*:B] - k_{dc}\cdot[D^*:B] + k^1_{sd}\cdot[S^*:B] \\
&\quad +k^1_{td}\cdot[T^*:B] + k_{di}\cdot[D^*:B:Ai] + k_{di}\cdot[D^*:B:Ai_2] \\
\frac{d[S^*:B]}{dt} &= k_{cat}\cdot[S:A:B] + k^1_{ds}\cdot[D^*:B] - k^1_{sd}\cdot[S^*:B] \\
&\quad -k^1_{su}\cdot[S^*:B] - k_{dc}\cdot[S^*:B] + k^1_{us}\cdot[U^*:B] \\
&\quad +k_{cbf}\cdot[S^*]\cdot[B] - k_{sai}\cdot[S^*:B]\cdot[A] - k_{sai}\cdot[S^*:B]\cdot[Ai_2] \\
\frac{d[T^*:B]}{dt} &= k_{cat}\cdot[T:A:B] + k^1_{dt}\cdot[D^*:B] - k_{cbr}\cdot[T^*:B] \\
&\quad -k^1_{td}\cdot[T^*:B] - k^1_{tu}\cdot[T^*:B] - k_{dc}\cdot[T^*:B] \\
&\quad +k^1_{ut}\cdot[U^*:B] + k_{di}\cdot[T^*:B:Ai] + k_{di}\cdot[T^*:B:Ai_2] \\
\frac{d[U^*:B]}{dt} &= k_{cat}\cdot[U:A:B] + k^1_{su}\cdot[S^*:B] + k^1_{tu}\cdot[T^*:B] \\
&\quad -k_{cbr}\cdot[U^*:B] - k^1_{us}\cdot[U^*:B] - k^1_{ut}\cdot[U^*:B] \\
&\quad -k_{dc}\cdot[U^*:B] + k_{di}\cdot[U^*:B:Ai] + k_{di}\cdot[U^*:B:Ai_2] \\
\frac{d[D:B:Ai]}{dt} &= -k_{cbr}\cdot[D:B:Ai] - k^0_{ds}\cdot[D:B:Ai] - k^0_{dt}\cdot[D:B:Ai] \\
&\quad -k_{di}\cdot[D:B:Ai] + k^0_{sd}\cdot[S:B:Ai] + k^0_{td}\cdot[T:B:Ai] \\
&\quad +k_{car}\cdot[D:A:B:Ai] + k_{dc}\cdot[D^*:B:Ai] + k_{di}\cdot[D:B:Ai_2] \\
&\quad -k_{caf}\cdot[D:B:Ai]\cdot[A] \\
\frac{d[S:B:Ai]}{dt} &= k^0_{ds}\cdot[D:B:Ai] - k^0_{sd}\cdot[S:B:Ai] - k^0_{su}\cdot[S:B:Ai] \\
&\quad +k^0_{us}\cdot[U:B:Ai] + k_{car}\cdot[S:A:B:Ai] + k_{dc}\cdot[S^*:B:Ai] \\
&\quad +k_{cbf}\cdot[S:Ai]\cdot[B] + k_{sai}\cdot[S:B]\cdot[A] - k_{caf}\cdot[S:B:Ai]\cdot[A] \\
&\quad -k_{sai2}\cdot[S:B:Ai]\cdot[A]
\end{aligned}
$$

$$
\begin{aligned}
\frac{d[T:B:Ai]}{dt} &= k^0_{dt}\cdot[D:B:Ai] - k_{cbr}\cdot[T:B:Ai] - k^0_{td}\cdot[T:B:Ai] \\
&\quad -k^0_{tu}\cdot[T:B:Ai] - k_{di}\cdot[T:B:Ai] + k^0_{ut}\cdot[U:B:Ai] \\
&\quad +k_{car}\cdot[T:A:B:Ai] + k_{dc}\cdot[T^*:B:Ai] + k_{di}\cdot[T:B:Ai_2] \\
&\quad -k_{caf}\cdot[T:B:Ai]\cdot[A] \\
\frac{d[U:B:Ai]}{dt} &= k^0_{su}\cdot[S:B:Ai] + k^0_{tu}\cdot[T:B:Ai] - k_{cbr}\cdot[U:B:Ai] \\
&\quad -k^0_{us}\cdot[U:B:Ai] - k^0_{ut}\cdot[U:B:Ai] - k_{di}\cdot[U:B:Ai] \\
&\quad +k_{car}\cdot[U:A:B:Ai] + k_{dc}\cdot[U^*:B:Ai] + k_{di}\cdot[U:B:Ai_2] \\
&\quad -k_{caf}\cdot[U:B:Ai]\cdot[A] \\
\frac{d[D:A:B:Ai]}{dt} &= -k_{cbr}\cdot[D:A:B:Ai] - k_{car}\cdot[D:A:B:Ai] - k^0_{ds}\cdot[D:A:B:Ai] \\
&\quad -k^0_{dt}\cdot[D:A:B:Ai] - k_{di}\cdot[D:A:B:Ai] - k_{cat}\cdot[D:A:B:Ai] \\
&\quad +k^0_{sd}\cdot[S:A:B:Ai] + k^0_{td}\cdot[T:A:B:Ai] + k_{di}\cdot[D:A:B:Ai_2] \\
&\quad +k_{caf}\cdot[D:B:Ai]\cdot[A] \\
\frac{d[S:A:B:Ai]}{dt} &= k^0_{ds}\cdot[D:A:B:Ai] - k_{car}\cdot[S:A:B:Ai] - k^0_{sd}\cdot[S:A:B:Ai] \\
&\quad -k^0_{su}\cdot[S:A:B:Ai] - k_{cat}\cdot[S:A:B:Ai] + k^0_{us}\cdot[U:A:B:Ai] \\
&\quad +k_{cbf}\cdot[S:A:Ai]\cdot[B] + k_{sai}\cdot[S:A:B]\cdot[A] + k_{caf}\cdot[S:B:Ai]\cdot[A] \\
&\quad -k_{sai2}\cdot[S:A:B:Ai]\cdot[A] \\
\frac{d[T:A:B:Ai]}{dt} &= k^0_{dt}\cdot[D:A:B:Ai] - k_{cbr}\cdot[T:A:B:Ai] - k_{car}\cdot[T:A:B:Ai] \\
&\quad -k^0_{td}\cdot[T:A:B:Ai] - k^0_{tu}\cdot[T:A:B:Ai] - k_{di}\cdot[T:A:B:Ai] \\
&\quad -k_{cat}\cdot[T:A:B:Ai] + k^0_{ut}\cdot[U:A:B:Ai] + k_{di}\cdot[T:A:B:Ai_2] \\
&\quad +k_{caf}\cdot[T:B:Ai]\cdot[A] \\
\frac{d[U:A:B:Ai]}{dt} &= k^0_{su}\cdot[S:A:B:Ai] + k^0_{tu}\cdot[T:A:B:Ai] - k_{cbr}\cdot[U:A:B:Ai] \\
&\quad -k_{car}\cdot[U:A:B:Ai] - k^0_{us}\cdot[U:A:B:Ai] - k^0_{ut}\cdot[U:A:B:Ai] \\
&\quad -k_{di}\cdot[U:A:B:Ai] - k_{cat}\cdot[U:A:B:Ai] + k_{di}\cdot[U:A:B:Ai_2] \\
&\quad +k_{caf}\cdot[U:B:Ai]\cdot[A]
\end{aligned}
$$

$$
\begin{aligned}
\frac{d[D^* : B : Ai]}{dt} &= k_{cat} \cdot [D : A : B : Ai] - k_{cbr} \cdot [D^* : B : Ai] - k^1_{ds} \cdot [D^* : B : Ai] \\
&\quad -k^1_{dt} \cdot [D^* : B : Ai] - k_{di} \cdot [D^* : B : Ai] - k_{dc} \cdot [D^* : B : Ai] \\
&\quad +k^1_{sd} \cdot [S^* : B : Ai] + k^1_{td} \cdot [T^* : B : Ai] + k_{di} \cdot [D^* : B : Ai_2] \\
\frac{d[S^* : B : Ai]}{dt} &= k_{cat} \cdot [S : A : B : Ai] + k^1_{ds} \cdot [D^* : B : Ai] - k^1_{sd} \cdot [S^* : B : Ai] \\
&\quad -k^1_{su} \cdot [S^* : B : Ai] - k_{dc} \cdot [S^* : B : Ai] + k^1_{us} \cdot [U^* : B : Ai] \\
&\quad +k_{cbf} \cdot [S^* : Ai] \cdot [B] + k_{sai} \cdot [S^* : B] \cdot [A] - k_{sai2} \cdot [S^* : B : Ai] \cdot [A] \\
\frac{d[T^* : B : Ai]}{dt} &= k_{cat} \cdot [T : A : B : Ai] + k^1_{dt} \cdot [D^* : B : Ai] - k_{cbr} \cdot [T^* : B : Ai] \\
&\quad -k^1_{td} \cdot [T^* : B : Ai] - k^1_{tu} \cdot [T^* : B : Ai] - k_{di} \cdot [T^* : B : Ai] \\
&\quad -k_{dc} \cdot [T^* : B : Ai] + k^1_{ut} \cdot [U^* : B : Ai] + k_{di} \cdot [T^* : B : Ai_2] \\
\frac{d[U^* : B : Ai]}{dt} &= k_{cat} \cdot [U : A : B : Ai] + k^1_{su} \cdot [S^* : B : Ai] + k^1_{tu} \cdot [T^* : B : Ai] \\
&\quad -k_{cbr} \cdot [U^* : B : Ai] - k^1_{us} \cdot [U^* : B : Ai] - k^1_{ut} \cdot [U^* : B : Ai] \\
&\quad -k_{di} \cdot [U^* : B : Ai] - k_{dc} \cdot [U^* : B : Ai] + k_{di} \cdot [U^* : B : Ai_2] \\
\frac{d[D : B : Ai_2]}{dt} &= -k_{cbr} \cdot [D : B : Ai_2] - k^0_{ds} \cdot [D : B : Ai_2] - k^0_{dt} \cdot [D : B : Ai_2] \\
&\quad -2 \cdot k_{di} \cdot [D : B : Ai_2] + k^0_{sd} \cdot [S : B : Ai_2] + k^0_{td} \cdot [T : B : Ai_2] \\
&\quad +k_{car} \cdot [D : A : B : Ai_2] + k_{dc} \cdot [D^* : B : Ai_2] - k_{caf} \cdot [D : B : Ai_2] \cdot [A] \\
\frac{d[S : B : Ai_2]}{dt} &= k^0_{ds} \cdot [D : B : Ai_2] - k^0_{sd} \cdot [S : B : Ai_2] - k^0_{su} \cdot [S : B : Ai_2] \\
&\quad +k^0_{us} \cdot [U : B : Ai_2] + k_{car} \cdot [S : A : B : Ai_2] + k_{dc} \cdot [S^* : B : Ai_2] \\
&\quad +k_{cbf} \cdot [S : Ai_2] \cdot [B] + k_{sai2} \cdot [S : B : Ai] \cdot [A] - k_{caf} \cdot [S : B : Ai_2] \cdot [A] \\
&\quad +k_{sai} \cdot [S : B] \cdot [Ai_2] \\
\frac{d[T : B : Ai_2]}{dt} &= k^0_{dt} \cdot [D : B : Ai_2] - k_{cbr} \cdot [T : B : Ai_2] - k^0_{td} \cdot [T : B : Ai_2] \\
&\quad -k^0_{tu} \cdot [T : B : Ai_2] - 2 \cdot k_{di} \cdot [T : B : Ai_2] + k^0_{ut} \cdot [U : B : Ai_2] \\
&\quad +k_{car} \cdot [T : A : B : Ai_2] + k_{dc} \cdot [T^* : B : Ai_2] - k_{caf} \cdot [T : B : Ai_2] \cdot [A] \\
\frac{d[U : B : Ai_2]}{dt} &= k^0_{su} \cdot [S : B : Ai_2] + k^0_{tu} \cdot [T : B : Ai_2] - k_{cbr} \cdot [U : B : Ai_2] \\
&\quad -k^0_{us} \cdot [U : B : Ai_2] - k^0_{ut} \cdot [U : B : Ai_2] - 2 \cdot k_{di} \cdot [U : B : Ai_2] \\
&\quad +k_{car} \cdot [U : A : B : Ai_2] + k_{dc} \cdot [U^* : B : Ai_2] - k_{caf} \cdot [U : B : Ai_2] \cdot [A]
\end{aligned}
$$

$$
\begin{aligned}
\frac{d[D:A:B:Ai_2]}{dt} &= -k_{cbr}\cdot[D:A:B:Ai_2] - k_{car}\cdot[D:A:B:Ai_2] \\
&\quad -k^0_{ds}\cdot[D:A:B:Ai_2] - k^0_{dt}\cdot[D:A:B:Ai_2] \\
&\quad -2\cdot k_{di}\cdot[D:A:B:Ai_2] - k_{cat}\cdot[D:A:B:Ai_2] \\
&\quad +k^0_{sd}\cdot[S:A:B:Ai_2] + k^0_{td}\cdot[T:A:B:Ai_2] \\
&\quad +k_{caf}\cdot[D:B:Ai_2]\cdot[A] \\
\frac{d[S:A:B:Ai_2]}{dt} &= k^0_{ds}\cdot[D:A:B:Ai_2] - k_{car}\cdot[S:A:B:Ai_2] \\
&\quad -k^0_{sd}\cdot[S:A:B:Ai_2] - k^0_{su}\cdot[S:A:B:Ai_2] \\
&\quad -k_{cat}\cdot[S:A:B:Ai_2] + k^0_{us}\cdot[U:A:B:Ai_2] \\
&\quad +k_{cbf}\cdot[S:A:Ai_2]\cdot[B] + k_{sai2}\cdot[S:A:B:Ai]\cdot[A] \\
&\quad +k_{caf}\cdot[S:B:Ai_2]\cdot[A] + k_{sai}\cdot[S:A:B]\cdot[Ai_2] \\
\frac{d[T:A:B:Ai_2]}{dt} &= k^0_{dt}\cdot[D:A:B:Ai_2] - k_{cbr}\cdot[T:A:B:Ai_2] \\
&\quad -k_{car}\cdot[T:A:B:Ai_2] - k^0_{td}\cdot[T:A:B:Ai_2] \\
&\quad -k^0_{tu}\cdot[T:A:B:Ai_2] - 2\cdot k_{di}\cdot[T:A:B:Ai_2] \\
&\quad -k_{cat}\cdot[T:A:B:Ai_2] + k^0_{ut}\cdot[U:A:B:Ai_2] \\
&\quad +k_{caf}\cdot[T:B:Ai_2]\cdot[A] \\
\frac{d[U:A:B:Ai_2]}{dt} &= k^0_{su}\cdot[S:A:B:Ai_2] + k^0_{tu}\cdot[T:A:B:Ai_2] \\
&\quad -k_{cbr}\cdot[U:A:B:Ai_2] - k_{car}\cdot[U:A:B:Ai_2] \\
&\quad -k^0_{us}\cdot[U:A:B:Ai_2] - k^0_{ut}\cdot[U:A:B:Ai_2] \\
&\quad -2\cdot k_{di}\cdot[U:A:B:Ai_2] - k_{cat}\cdot[U:A:B:Ai_2] \\
&\quad +k_{caf}\cdot[U:B:Ai_2]\cdot[A] \\
\frac{d[D^*:B:Ai_2]}{dt} &= k_{cat}\cdot[D:A:B:Ai_2] - k_{cbr}\cdot[D^*:B:Ai_2] - k^1_{ds}\cdot[D^*:B:Ai_2] \\
&\quad -k^1_{dt}\cdot[D^*:B:Ai_2] - 2\cdot k_{di}\cdot[D^*:B:Ai_2] - k_{dc}\cdot[D^*:B:Ai_2] \\
&\quad +k^1_{sd}\cdot[S^*:B:Ai_2] + k^1_{td}\cdot[T^*:B:Ai_2]
\end{aligned}
$$

$$
\begin{aligned}
\frac{d[S^* : B : Ai_2]}{dt} &= k_{cat} \cdot [S : A : B : Ai_2] + k^1_{ds} \cdot [D^* : B : Ai_2] - k^1_{sd} \cdot [S^* : B : Ai_2] \\
&\quad -k^1_{su} \cdot [S^* : B : Ai_2] - k_{dc} \cdot [S^* : B : Ai_2] + k^1_{us} \cdot [U^* : B : Ai_2] \\
&\quad +k_{cbf} \cdot [S^* : Ai_2] \cdot [B] + k_{sai2} \cdot [S^* : B : Ai] \cdot [A] + k_{sai} \cdot [S^* : B] \cdot [Ai_2] \\
\frac{d[T^* : B : Ai_2]}{dt} &= k_{cat} \cdot [T : A : B : Ai_2] + k^1_{dt} \cdot [D^* : B : Ai_2] - k_{cbr} \cdot [T^* : B : Ai_2] \\
&\quad -k^1_{td} \cdot [T^* : B : Ai_2] - k^1_{tu} \cdot [T^* : B : Ai_2] - 2 \cdot k_{di} \cdot [T^* : B : Ai_2] \\
&\quad -k_{dc} \cdot [T^* : B : Ai_2] + k^1_{ut} \cdot [U^* : B : Ai_2] \\
\frac{d[U^* : B : Ai_2]}{dt} &= k_{cat} \cdot [U : A : B : Ai_2] + k^1_{su} \cdot [S^* : B : Ai_2] + k^1_{tu} \cdot [T^* : B : Ai_2] \\
&\quad -k_{cbr} \cdot [U^* : B : Ai_2] - k^1_{us} \cdot [U^* : B : Ai_2] - k^1_{ut} \cdot [U^* : B : Ai_2] \\
&\quad -2 \cdot k_{di} \cdot [U^* : B : Ai_2] - k_{dc} \cdot [U^* : B : Ai_2]
\end{aligned}
$$

Bibliography

[1] Alan Aderem. Systems Biology: Its Practices and Challenges. *Cell*, 121(4):511–513, May 2005.

[2] Shuji Akiyama, Atsushi Nohara, Kazuki Ito, and Yuichiro Maéda. Assembly and Disassembly Dynamics of the Cyanobacterial Periodosome. *Molecular Cell*, 29(6):703–716, March 2008.

[3] Minna Allarakhia and Anthony Wensley. Systems biology: A disruptive biopharmaceutical research paradigm. *Technological Forecast and Social Change*, 74(9):1642–1660, November 2007.

[4] Ernesto Andrianantoandro, Subhayu Basu, David K. Karig, and Ron Weiss. Synthetic biology: new engineering rules for an emerging discipline. *Molecular Systems Biology*, 2(2006.0028), May 2006.

[5] Joshua F. Apgar, Jared E. Toettcher, Jacob W. White, and Bruce Tidor. KroneckerBio v1.0.0 alpha. Software licensed under MIT.

[6] Peter Bringmann, Eugene C. Butcher, Gordon Parry, and Bertram Weiss. *Systems biology: applications and perspectives.* Springer, 2007.

[7] Frank J. Bruggeman and Hans V. Westerhoff. The nature of systems biology. *Trends in Microbiology*, 15(1):45–50, November 2006.

[8] Marvin Cassman. Systems biology: Executive Summary and Introduction. *Springer*, 2007.

[9] Colin Dollery, Richard Kitney, Richard Challis, David Delpy, David Edwards, Adriano Henney, Tom Kirkwood, Denis Noble, Malcolm Rowland, Lionel Tarassenko, and David Williams. Systems Biology: a vision for engineering and medicine. *The Academy of Medical Sciences and The Royal Academy of Engineering*, February 2007.

[10] Claus Emmeche. *Defining Life, Explaining Emergence.* Niels Bohr Institute, 1997.

[11] Iman Famili and Bernhard O. Palsson. The Convex Basis of the Left Null Space of the Stoichiometric Matrix Leads to the Definition of Metabolically Meaningful Pools. *Biophysical Journal*, 85:16–26, July 2003.

[12] Jasmin Fisher. *Formal Methods in Systems Biology.* Springer, 2008.

[13] Pengcheng Fu, Martin Latterich, and Sven Panke. *Systems Biology and Synthetic Biology.* John Wiley and Sons, 2009.

[14] Herbert Gutfreund. *Kinetics for the life sciences: receptors, transmitters, and catalysts.* Cambridge University Press, 1995.

[15] Stacey L. Harmer, Satchidananda Panda, and Steve A. Kay. Molecular Bases of Circadian Rhythms. *Annual Review of Cell and Developmental Biology*, 17:215–253, November 2001.

[16] Antonia Herrero and Enrique Flores. *The Cyanobacteria: Molecular Biology, Genomics and Evolution.* Horizon Scientific Press, 2008.

[17] Leroy Hood. Systems biology: integrating technology, biology, and computation. *Mechanisms of Ageing and Devleopment*, 124:9–16, January 2003.

[18] Trey Ideker, Timothy Galitski, and Leroy Hood. A New Approach to Decoding Life: Systems Biology. *Annual Review of Genomics and Human Genetics*, 2:343–372, September 2001.

[19] Hiroshi ito, Hakuto Kageyama, Michinori Mutsuda, Masato Nakajima, Tokitaka Oyama, and Takao Kondo. Autonomous synchronization of the circadian KaiC phosphorylation rhythm. *Nature Structural and Molecular Biology*, 14(11):1084–1088, November 2007.

[20] Sheila S. Jasanoff. Contested Boundaries in Policy-Relevant Science. *Social Studies of Science*, 17(2):195–230, May 1987.

[21] Carl Hirchie Johnson, Martin Egli, and Phoebe L. Stewart. Structural Insights into a Circadian Oscillator. *Science*, 322(5902):697–701, October 2008.

[22] Hakuto Kageyama, Hideo Iwasaki, and Takao Kondo. Circadian formation of clock protein complexes by KaiA, KaiB, KaiC, and SasA in cyanobacteria. *J. Biol. Chem.*, 278(4):2388–2395, November 2003.

[23] Hakuto Kageyama, Taeko Nishiwaki, Masato Nakajima, Hideo Iwasaki, Tokitaka Oyama, and Takao Kondo. Cyanobacterial Circadian Pacemaker: Kai Protein Complex Dynamics in the KaiC Phosphorylation Cycle *In Vitro*. *Molecular Cell*, 23(2):161–171, July 2006.

[24] Yong-Ick Kim, Guogang Dong, Carl W. Carruthers Jr, Susan S. Golden, and Andy LiWang. The day/night switch in KaiC, a central oscillator component of the circadian clock of cyanobacteria. *Proc. Natl. Acad. Sci. USA*, 105(35):12825–12830, September 2008.

[25] Hiroaki Kitano. *Foundations of Systems Biology.* MIT Press, 2001.

[26] E. Klipp, R. Herwig, A. Kowald, C.Wierling, and H. Lehrach. *Systems Biology in Practice: Concepts, Implementation, and Application.* WILEY-VCH, 2005.

[27] Wayne Materi and David Wishart. Computational systems biology in drug discovery and development: methods and applications. *Nature Structural and Molecular Biology*, 12(7-8):295–303, April 2007.

[28] Tetsuya Mori, Sergei V. Saveliev, Yao Xu, Walter F. Stafford, Michael M. Cox, Ross B. Inman, and Carl H. Johnson. Circadian clock protein KaiC forms ATP-dependent hexameric rings and binds DNA. *Proc. Natl. Acad. Sci. USA*, 99(26):17203–17208, December 2002.

[29] Tetsuya Mori, Dewight R. Williams, Mark O. Byrne, Ximing Qin, Martin Egli, Hassane S. Mchaourab, Phoebe L. Stewart, and Carl Hirschie Johnson. Elucidating the Ticking of an *In Vitro* Circadian Clockwork. *PLoS Biol*, 5(4):e93, April 2007.

[30] James Dickson Murray. *Mathematical biology.* Niels Bohr Institute, 1997.

[31] Masato Nakajima, Keiko Imai, Hiroshi Ito, Taeko Nishiwaki, Yoriko Murayama, Hideo Iwasaki, Tokitaka Oyama, and Takao Kondo. Reconstitution of Circadian Oscillation of Cyanobacterial KaiC Phosphorylation *in Vitro*. *Science*, 308(5720):414–415, April 2005.

[32] Taeko Nishiwaki, Hideo Iwasaki, Masahiro Ishiura, and Takao Kondo. Nucleotide binding and autophosphorylation of the clock protein KaiC as a circadian timing process of cyanobacteria. *Biophysical Journal*, 97:495–499, January 2000.

[33] Taeko Nishiwaki, Yoshinori Satomi, Yohko Kitayama, Kazuki Terauchi, Reiko Kiyohara, Toshifumi Takao, and Takao Kondo. A sequential program of dual phosphorylation of KaiC as a basis for circadian rhythm in cyanibacteria. *The EMBO Journal*, 26(17):4029–4037, August 2007.

[34] Taeko Nishiwaki, Yoshinori Satomi, Masato Nakajima, Cheolju Lee, Reiko Kiyohara, Hakuto Kageyama, Yohko Kitayama, Mioko Temamoto, Akihiro Yamaguchi, Atsushi Hijikata, Mitiko Go, Kideo Iwasaki, Toshifumi Takao, and Takao Kondo. Role of KaiC phosphorylation in the circadian clock system of Synechococcus elongatus PCC 7942. *Proc. Natl. Acad. Sci. USA*, 101(38):13927–13932, September 2004.

[35] M. O'Malley, J. Calvert, and J. Dupré. The study of socioethical issues in systems biology. *The American Journal of Bioethics*, 7(4):67–78, 2007.

[36] Arti K. Rai. Open and collaborative research: A new model for biomedicine. *Intellectual Property Rights in Frontier Industries: Software and Biotech*, 2004.

[37] Marc H.V. Van Regenmortel. Reductionism and complexity in molecular biology. *Science and Society*, November 2004.

[38] J.S. Robert, J. Maienschein, and M.D. Laubichler. Systems Bioethics and Stem Cell Biology. *Journal of Bioethical Inquiry*, 3:19–31, 2006.

[39] Jr Roger A. Pielke. Science policy: Policy, politics and perspective. *Nature*, 416:367–368, March 2002.

[40] Michael J. Rust, Joseph S. Markson, William S. Lane, Daniel S. Fisher, and Erin K. O'Shea. Ordered Phosphorylation Governs Oscillation of a Three-Protein Circadian Clock. *Science*, 318:809–812, October 2007.

[41] Lee A. Segel. *Mathematical models in molecular and cellular biology.* CUP Archive, 1980.

[42] Thomas Traut. *Allosteric Regulatory Enzymes.* Springer, 2007.

[43] P. Vallance and T.G. Smart. The future of pharmacology. *British Journal of Pharmacology*, 147:S304–S307, 2006.

[44] J.A.C Weideman. Numerical Integration of Periodic Functions: A Few Examples. *American Mathematical Monthly*, 109:21–36, January 2002.

[45] Anna Katharina Wilkins. *Sensitivity analysis of oscillating dynamical systems with applications to the mammalian circadian clock.* PhD dissertation, Massachusetts Institute of Technology, Department of Chemical Engineering, 2008.

[46] Yao Xu, Tetsuya Mori, and Carl Hirschie Johnson. Cyanobacterial circadian clockwork: roles of KaiA, KaiB, and *kaiBC* promoter in regulating KaiC. *EMBO*, 22(9):2117–2126, 2003.

[47] Yao Xu, Tetsuya Mori, Rekha Pattanayek, Sabuj Pattanayek, and Martin Egli. Identification of key phosphorylation sites in the circadian clock protein KaiC by crystallographic and mutagenetic analyses. *Proc. Natl. Acad. Sci. USA*, 101(38):13933–13938, September 2004.

[48] Sheng Ye, Ioannis Vakonakis, Thomas R. Ioerger, and Andy C. LiWang. Crystal Structure of Circadian Clock Protein KaiA from *Synechococcus elongatus*. *The Journal of Biological Chemistry*, 279(19):20511–20518, May 2004.